NON-DARCIAN FLOW THROUGH ROCKFILLS

A THESIS SUBMITTED TO
THE GRADUATE SCHOOL OF NATURAL AND APPLIED SCIENCES
OF
MIDDLE EAST TECHNICAL UNIVERSITY

BY

ÖZGE KÜREKSİZ

IN PARTIAL FULFILLMENT OF THE REQUIREMENTS
FOR
THE DEGREE OF MASTER OF SCIENCE
IN
CIVIL ENGINEERING

JULY 2008

Approval of the thesis:

NON-DARCIAN FLOW THROUGH ROCKFILLS

Submitted by **ÖZGE KÜREKSİZ** in partial fulfillment of the requirements for the degree of **Master of Science in Civil Engineering Department, Middle East Technical University** by,

Prof. Dr. Canan Özgen
Dean, Graduate School of **Natural and Applied Sciences** _____

Prof. Dr. Güney Özcebe
Head of Department, **Civil Engineering Dept., METU** _____

Prof. Dr. Halil Önder
Supervisor, **Civil Engineering Dept., METU** _____

Examining Committee Members

Prof. Dr. Mustafa Göğüş
Civil Engineering Dept., METU _____

Prof. Dr. Halil Önder
Supervisor, Civil Engineering Dept., METU _____

Assoc. Dr. A.Burcu Altan Sakarya
Civil Engineering Dept., METU _____

Asst. Dr. Şahnaz Tiğrek
Civil Engineering Dept., METU _____

Assoc. Dr. Mehmet Ali Kökpınar
Civil Engineer, DSI _____

Date: 29 July 2008

I hereby declare that all information in this document has been obtained and presented in accordance with academic rules and ethical conduct. I also declare that, as required by these rules and conduct, I have fully cited and referenced all material and results that are not original to this work.

Name, Last name: Özge KÜREKSİZ

Signature :

ABSTRACT

NON-DARCIAN FLOW THROUGH ROCKFILLS

Küreksiz, Özge

M.S., Department of Civil Engineering

Supervisor: Prof. Dr. Halil Önder

July 2008, 92 pages

An impermeable weir constructed across a stream prevents the longitudinal movement of aquatic life and transportation of physical and chemical substances in water, eventually having a negative impact on river environment. However, a rubble mound weir is considered environmentally friendly, since its permeability allows the streamwise migration of aquatic life. This thesis investigates the performance of this type of weir as a water use facility. The particular objective of the investigation is to study the flow mechanism in terms of water surface profile and discharge through the weir. In the study, flow through the rubble mound weir is considered non-Darcian, steady, and one-dimensional. In the analysis, gradually varied open channel flow algorithm is applied to porous medium flow through the rubble mound weir in which laminar and turbulent components of flow are taken into consideration. Unlike previous studies where Stephenson and Wilkins relations were used, in this thesis Forchheimer equation is used. To verify the validity of numerical solution of governing equation based on Forchheimer relation, an experimental investigation is conducted in the laboratory. The experimentally obtained water surface profiles are compared with the numerical results. It is

observed that there is a satisfactory agreement between numerical and experimental results. The water surface profiles obtained by numerical solution are further compared with those based on Stephenson and Wilkins relations. It is concluded that the proposed numerical solution technique for the Forchheimer based governing equation may be used in the analysis of flow through, and design of rockfill weirs.

Keywords: Non-Darcian flow, Forchheimer equation, gradually varied flow, water surface profile, rockfill

ÖZ

DARCY KANUNA UYMAYAN TAŞ DOLGU İÇİNDEKİ AKIM

Küreksiz, Özge

Yüksek Lisans, İnşaat Mühendisliği Bölümü

Tez Yöneticisi : Prof. Dr. Halil Önder

Temmuz 2008, 92 sayfa

Geçirimsiz seddeler nehir sularından değişik amaçlarla yararlanmak ve gerekli kontrolü sağlamak için sık sık kullanılmaktadırlar. Bu tür yapılar akarsuyun doğal akımını engellemekte akarsuyun kendi kendini temizleme yeteneğini azaltmaktadırlar. Nehrin akışaşağı ve akışyukarı bölümleri arasında bir engel oluşturarak doğal yaşam ortamını olumsuz yönde etkilemektedirler. Bu nedenlerle son yıllarda daha çevre dostu olan geçirimli taş dolgu yapılar göz önüne alınmaktadır. Bu çalışmanın amacı bir taş dolgu bent içinde oluşan tek boyutlu, Darcy Kanunu'na uymayan akımın su yüzü profilini sayısal yöntemle hesaplamaktır. Burada yalnızca gözenekli ortam içindeki akım ele alınmış olup bend üzerindeki akımın olmadığı durum düşünülmüştür. Dolgu içerisindeki su yüzü profilini hesaplamak için yavaş değişen açık kanal akımı algoritması kullanılmıştır. Bu algoritmada gerekli olan enerji çizgisi eğimi için, gözenekli ortamlarda yaygın olarak kullanılan Forchheimmer denklemi kullanılmıştır. Bu denklem sayesinde laminar ve türbülanslı akım koşulları göz önüne alınmış bulunmaktadır. Bu tezde elde edilen su yüzey profilleri daha önceki çalışmalarda kullanılan Stephenson ve Wilkins denklemlerine dayanan hesap sonuçları ile kıyaslanmıştır. Ayrıca, önerilen

sayısal çözümün geçerliliği laboratuvar koşullarında yapılan deneysel çalışma sonuçları ile kıyaslanarak, sayısal yöntemin geçerliliğinin doğrulanması hedeflenmiştir. Deney sonuçlarının Forchheimer denklemine dayanan sayısal çözüm ile makul bir uyumluluk içerisinde olduğu görülmüştür. Önerilen sayısal çözüm tekniğinin dolgu içerisindeki akım analizinde ve su bendi tasarımında kullanılabileceği sonucuna varılmıştır.

Anahtar Kelimeler: Darcy kanununa uymayan akım, Forchheimer bağıntısı, yavaş değişen akım, su yüzü profili, taş dolgu

ACKNOWLEDGMENTS

I would like to express my deepest gratitude to my supervisor Prof. Dr. Halil Önder for his guidance, encouragement, advice, criticism, and insight throughout the research.

I would specially like to express my thanks to my sister Funda Küreksiz for her useful discussions and patience. I would also like to thank my father A.Kadir Küreksiz and mother Seyide Küreksiz for their moral support.

In addition, I would like to express my deepest thanks to research assistants Meriç Selamoğlu and Ö.İlker Küçüktepe, and my best friend Ürün Bakar for their encouragements and advice.

I would kindly like to thank to Middle East Technical University Civil Engineering Department Hydromechanics Laboratory for supplying experimental investigation conditions.

I am also grateful to the staff of the Hydromechanics Laboratory, Turgut Ural, Cengiz Tufaner, and Hüseyin Gündoğdu for their helps.

To my parents and my sister for their endless love, patience and support

TABLE OF CONTENTS

LIST OF TABLES

TABLES

LIST OF FIGURES

FIGURES

LIST OF SYMBOLS

A	: Cross-sectional area
A_1 & A_2	: Empirically or theoretically determined constants
$b_{channel}$	: Width of the channel
b_{weir}	: Width of the weir
c	: Dimensionless coefficient related to drag force acting on a particle
c_1 & c_2	: Integration constants
C_d	: Discharge coefficient
d	: Particle diameter
D	: Hydraulic depth
Fr_p	: Pore Froude number
g	: Gravitational acceleration
h	: Piezometric head
h_{weir}	: Height of the weir
H	: Total head
i	: Discrete number
I	: Hydraulic gradient

j : Iteration number

k : Geometric permeability

K : Hydraulic conductivity

K_{st} : Stephenson friction factor

K_t : Parameter to account for the angularity of the particles

L : Length

L_l : Effective length of the crest

$L_{channel}$: Length of the channel

L_{weir} : Length of the weir

m : Hydraulic mean radius of the coarse porous media

m' : Slope of water table

M : Total number of cross-sections in the reach being considered

n : Porosity

P : Pressure

P' : Height of weir used for discharge measurement

q : Specific discharge

Q : Discharge

Q_b : Discharge per unit width

Re : Pore Reynolds number

R^2 : Root mean square value

S_0 : Bed slope of channel

S_f : Friction slope

V : Average velocity

W : Wilkins constant

x : Longitudinal coordinate originated at upstream boundary of weir

y : Vertical water depth

y_p : Piezometric water depth

$\dot{y}$: Differential of y with respect to x

z : Elevation head

Z : Measured water head over the crest

α : Slope of equation (4.7)

γ : Specific weight of fluid

ν : Kinematic viscosity of fluid

θ : Stream bed angle

$\forall_{total}$: Total volume of the weir

$\forall_{brick}$: Total volume of bricks

$\forall_{void}$: Volume of void

CHAPTER 1

INTRODUCTION

1.1 Introduction and Statement of Problem

Weirs, embankments, and rockfill structures are used frequently in order to create a reservoir for water supply and irrigation or to arrange the river flow for flood control purposes. In recent decades, an emphasis is given on the sustainable use of water resources and ecologically friendly solution in various disciplines.

An impermeable weir constructed across a stream prevents the longitudinal movement of aquatic life and transportation of physical and chemical substances in water, eventually having a negative impact on the river environment. Therefore, it is not considered as an ecologically friendly structure.

Nevertheless, the rubble mound weir allows the streamwise migration of aquatic life, because the body is porous and the slope on the downstream side is mild. In this manner, the structure may also serve the function of fish ladder or fish way. Minor modifications to the structure, such as the installation of a mild slope spillway, are expected to improve its performance as a fish ladder. From the viewpoint of water quality, physical and chemical substances such as sediments and suspended organic matter can pass downstream through the permeable body. This eventually minimizes sedimentation and eutrophication in the impoundment behind the weir.

In connection with the above issues, as compared to the conventional impermeable weirs constructed of materials such as concrete, the permeable rubble mound weir might serve a structure with minimal negative impact on the river environment and it is more environmentally friendly. However, available information of flow through permeable weirs is insufficient; thus, water surface profiles through these structures should be predicted for design of that kind of structures. The numerical model accompanied by analytical and/or physical model is the tool to serve this purpose.

1.2 Objectives of the Thesis

The main objective of this study is to simulate water surface profiles for one-dimensional non-Darcian flow through the rubble mound weir as a function of parameters such as discharge, porosity, grain diameter, and geometrical dimensions of the structure. Focus here is placed on ordinary flow conditions, where the flow takes place only through the rubble mound weir. The analysis of flow over the weir is excluded in this research work. In order to analyze the water surface profile, gradually varied flow algorithm is applied by considering porous medium flow through the rubble mound weir.

A one-dimensional analysis on a steady non-uniform flow is performed to obtain numerical solutions for water surface profile, in which laminar and turbulent components of flow resistance in the porous body are taken into consideration. While computing the profiles regarding these situations mentioned above, for the evaluation of friction slope Forchheimer Equation is used, unlike previous studies where Stephenson's and Wilkins' equations were used.

The other objective of this thesis is to verify the validity of the proposed numerical solution of Forchheimer relation based governing equation, by using an experimental investigation. The experimentally obtained water surface profiles are further compared with the numerical results.

1.3 Description of Thesis

This thesis is composed of six chapters.

In Chapter 1, an introduction and the objectives of this thesis are presented.

The literature survey on the subject matter and the mathematical formulation of the problem are given in Chapter 2. The governing equations that will be used in this study are derived in this section.

The numerical method to solve the governing equation is provided in Chapter 3.

In Chapter 4, the experimental setup is described. Experimental procedure and conducted experiments are presented.

The results from experimental and numerical studies are compared and discussed in Chapter 5. In addition, the results of the numerical study with additional test cases are given.

In Chapter 6, a brief summary on the performed study is given. This chapter contains a set of concluding remarks together with recommendations for future works.

In the Appendix A, the numerical data of the experimental study, all water head elevations obtained by numerical method, and related graphs are provided.

In Appendix B, photographs of experimental setup are presented.

CHAPTER 2

THEORETICAL BACKGROUND

This chapter starts with the summary of literature investigation. It is followed by a justification of the study. Then, according to the literature survey part, Darcy and non-Darcian flow equations are explained in detail. In the last part of this chapter, the final form of the governing equations is summarized.

2.1 Literature Survey

In recent studies, for simulation of water surface profiles, gradually varied flow algorithm is applied by considering porous medium flow through the rubble mound weir. Theoretical descriptions of the open channel flow have already been established and can be referred to mostly in well-known textbooks and publications such as Chow (1959), and French (1986). Similarly, general information on porous media flow is given in textbooks; for example, Bear (1979), Stephenson (1979), Todd (2005), and Vafai (2000).

Several disciplines have made important contributions to the development of models characterizing flow through porous media, among them groundwater hydrology, chemical engineering, petroleum engineering, and water treatment engineering. Theory of this flow is largely based on experimental work and theoretical analysis published by Henry Darcy, the engineer responsible for the water system in Lion, France, in the mid-19^{th} century (Trussell and Chang, 1999). Darcy's law is valid when the velocity is very small. Therefore, kinetic energy of the flow is negligible. However, there are occasions when the flow is non-Darcian.

Following Darcy, developments in the understanding of flow through porous media took two parallel but more or less independent tracks. The first track was led by hydro geologists, petroleum engineers, and civil engineers interested in characterizing the flow of various fluids (oil, gas, and water) in the underground environment. Civil engineers and chemical engineers, who are focused on predicting the head loss in engineered media, led the second track. In this case, a design engineer specifies the characteristics of the material that makes up the porous bed (Trussell and Chang, 1999).

One of the first was Forchheimer (1901), an early German investigator who demonstrated conditions under which the relationship between flow and head loss in porous media does not follow the simple linear relationship specified by Darcy. Another was Nutting (1930), who defined the specific resistance, a parameter similar to Darcy's coefficient, but corrected for the characteristics of the fluid. Shortly thereafter Wyckoff (1933) popularized Nutting's specific resistance parameter, resulting in its wide use whenever the modeling of the flow of fluids underground was undertaken. Also important were Scheidegger (1960), Hubbert (1956), Irmay (1958), Sunada (1965), Ahmed and Sunada (1969), and others who worked to show that Forchheimer's nonlinear equation could be derived from the Navier-Stokes equations.

Notable among investigators on the second track were Kozeny (1927a, 1927b), Fair and Hatch (1933), and Carman (1937), who developed a powerful model for predicting Darcy resistance from the characteristics of the porous media. In addition to those researches, Blake (1923) and Burke and Plummer (1928) applied similar principles to characterize the nonlinear resistance of porous media to the flow of gases at high Reynolds numbers. Moreover, Ergun and Orning (1949), and Ergun (1952) combined the linear and nonlinear models to produce one comprehensive model of porous media flow appropriate for a wide range of Reynolds numbers (Trussell and Chang, 1999).

As it is mentioned before, fluid flow through a rock fracture was usually assumed to obey a Darcy-like equation, a linear relationship between the flux and the pressure gradient. However, it is known that, at sufficiently high values of the Reynolds number, this relationship becomes nonlinear. Unfortunately, the complexity and irregularity of the geometry of rock fractures makes it difficult to quantify the onset of nonlinearity, or the precise algebraic form of the nonlinear relationship between flowrate and pressure drop (Zimmerman et al., 2004)

In literature, commonly used non-Darcian resistance laws are grouped under two forms, a quadratic type and a power type. Quadratic type is a well-known Forchheimer relation and the other one is the so-called Izbash equation. Many researchers have worked theoretically and experimentally to determine functional dependencies of constants in both quadratic and power type equations on relating parameters. Some of better-known non-Darcian flow equations are the Ergun equation and the Ergun-Reichelt equation (Bari and Hansen, 2002), the Martins equation (Martins, 1990), the McCorquodale equation (McCorquodale et al., 1978), Ward equation (Ward, 1964), the Stephenson equation (Stephenson, 1979), the Wilkins equation (Bari and Hansen, 2002). Among the non-Darcy flow equations mentioned above, the Stephenson's and the Wilkins' equations are the simplest in form and are widely used. Ward (1964) is one of those who successfully used a dimensional argument and proposed an equation that is the version of Forchheimer relation. In the study of Hansen et al. (1994), brief information about the non-Darcian flow equations is presented.

In order to analyze the flow through rockfill structure constructed on river, open channel flow and porous medium flow should be considered simultaneously. In Bari and Hansen (2002), calculation of water surface profiles of gradually varied flow was done by using Wilkins and Stephenson's equations. In that work, the longitudinal variation in water depth is no longer partly governed by the roughness of the streambed, as in the case for open channel flow, but by the characteristics of the coarse porous media. For non-Darcian flow through buried streams, friction slope is evaluated using Stephenson and Wilkins' equations. The numeric solutions were obtained by replacing friction slope with hydraulic gradient in that work with the application of a numerical scheme used by Prasad (1970).

In addition to these studies, non-Darcian flow through porous medium was provided in the study of Michioki et al. (2005) by using open channel flow approach. Main objective of this study was to formulate the discharge through a permeable rubble mound weir. In order to achieve this objective, Ward (1964) assumption was used. Unlike the previously mentioned work (Bari and Hansen, 2002), integration of governing differential equation was performed analytically instead of using numerical method as in Prasad (1970). Besides, hydraulic characteristics of a rubble mound weir were analyzed and summarized in the study of Maeno et al. (2002) with the help of experimental investigation. By considering these studies, water surface profile through rubble mound weir was analyzed numerically by using Forchheimer equation in the work of Kureksiz and Onder (2007). A set of experimental results are given in Kureksiz and Onder (2008).

The study of Li et al. (1998) also describes a synthesis of various studies on non-Darcian flow in rockfill material. Knowledge of the relationship between the velocity and the hydraulic gradient is essential for engineering design of flow through and over rockfill structures. By the help of pipe theory and Taylor's definition for mean hydraulic radius (Taylor, 1948), theoretical relationships between friction coefficient and Reynolds number and relationships between hydraulic gradient and bulk seepage velocity have been obtained in Li et al. (1998).

Regarding the fluid flow through rock fractures, in the study of Zimmerman et al. (2004) high-resolution Navier-Stokes simulations and laboratory measurements of fluid flow in a natural sandstone fracture have been conducted. That study leads to the conclusion that nonlinear effects should become appreciable at Reynolds numbers on the order of 10. At higher Reynolds numbers, a Forchheimer flow regime in which the pressure drop is given by a term that is linear in the flowrate (or Reynolds number), plus a term that depends quadratically on the flowrate is observed in both the simulations and the experiments.

2.1.1 Conclusion of Literature Survey

In the literature, there are few studies on flow through porous media in general, and rockfills in particular that incorporate non-Darcian flow conditions with open channel flow principles. It is explained in the objective part of thesis that aim of this thesis is to simulate the water surface profile of that kind of fluid flow. It can be concluded from literature survey that there are turbulent flow situations in nature, which means non-linear and non-Darcian. Analytical solution for quadratic type of equation can be troublesome even impossible to solve. Therefore, a numerical solution applicable to flow through porous media is required as an alternative. In the light of this necessity, the water surface profiles are analyzed and simulated numerically in this thesis. Moreover, in order to verify the numerical modeling of water surface profiles an experimental work is done.

2.2 Darcy's Law

The theory of flow through porous media was originated by Henry Darcy as an empirical relationship after his experimental studies. Darcy observed that the flow through a bed of filter sand was directly proportional to the hydraulic (piezometric) head acting on the sand bed and inversely proportional to its depth (Darcy, 1856).

Thoroughly, he concluded that the rate of flow, Q, is proportional to the cross-sectional area, A, and the piezometric head difference, $\Delta h = h_u - h_d$, and inversely proportional to the length, L, of the porous medium. These inferences gave the famous Darcy's formula:

$$Q = \frac{KA\Delta h}{L} \tag{2.1}$$

where K is the coefficient of proportionality.

Piezometric head measured with respect to some arbitrary horizontal datum, h, is expressed as

$$h = z + \frac{P}{\gamma} \tag{2.2}$$

where z is elevation head, P is the pressure, and P/γ is the pressure head.

Given that the piezometric head describes the sum of pressure and potential energies of the fluid per unit weight, $\Delta h/L$ is to be interpreted as hydraulic gradient. Denoting this gradient by I

$$Q = KAI \tag{2.3}$$

Defining the specific discharge, q, as the volume of water flowing per unit time through a unit cross-sectional area normal to the direction of flow, $q = Q/A$ .Then,

$$q = KI \tag{2.4}$$

Similarly,

$$q = \frac{K(h_u - h_d)}{L} \tag{2.5}$$

is another form of the Darcy's formula. Here, subscripts u and d refer the piezometric heads at upstream and downstream, respectively.

Darcy's linear law may also be extended to flow through an inclined homogenous column of porous medium (Bear, 1979). The range of validity of Darcy's law is that Reynolds number is less than 1 – 10 (Bear, 1979).

An energy loss exists due to friction in the flow through the parts of the porous media. In Darcy's law, the kinetic energy of fluid has been neglected because; in general, changes in the piezometric head along the flow path are much greater than the changes in kinetic energy. It is important to note that the flow takes place from a higher piezometric head to a lower head and not from a higher to lower pressure.

The flow takes place only through the void space of the cross-sectional area of the column of porous medium, the remaining part being occupied by the solid matrix of the porous medium. Since it can be shown that the average areal porosity is equal to the volumetric porosity, n, the portion of the area, A, available for flow is the product of the two that is nA. Accordingly, the real average velocity, V, of the flow through the column is

$$V = \frac{Q}{nA} = \frac{q}{n} \tag{2.6}$$

The coefficient of proportionality, K, appearing in Darcy's law is called the hydraulic conductivity of the porous medium. It depends on properties of both the porous matrix and the fluid.

2.3 Non-Darcian Flow

When Darcy originally proposed his relationship in 1856, it was intended to address the linear flow through filter sand. One-dimensional Darcian flow provides a good approximation of observed phreatic surface profile at low flow rates. Before long, it became clear that the actual head loss was often greater than that derived from Darcy's law, particularly when high flow velocities and coarse media were involved. As flow rate and hydraulic gradient increase, the strength of turbulent eddies within the material increases, providing additional resistance to flow

(Bordier and Zimmer, 2000). As a result, the Darcian flow model underestimates hydraulic gradient for higher flow rates. In literature, to solve this problem some non-Darcian resistance laws are proposed. Most widely used ones are grouped under two forms as a quadratic type and a power type as discussed in literature survey part.

In accordance with the explanation above, the non-linearity of the relationship between hydraulic gradient and Darcy velocity may be represented using a power law relationship of the form:

$$I = Cq^N \tag{2.7}$$

where C and N are the model parameters depending on characteristics of porous medium, flow condition, and the fluid. This relationship is mostly referred to as Izbash law and is empirically based.

In literature, a lot of alternatives for Izbash' flow equation are present. By analogy to flow in conduits, Stephenson (1979) proposed a form of Izbash equation that the hydraulic gradient for flow through coarse porous media might be expressed as;

$$I = \frac{K_{st}}{gd} q^2 \tag{2.8}$$

where, $C = K_{st} / gd$, and $N = 2$, are replaced in Equation (2.7).

In Equation (2.8), the parameter d represents particle diameter, g is the gravitational acceleration, and K_{st} is known as Stephenson's friction factor.

Moreover, Stephenson (1979) presented the following relation to evaluate K_{st} ;

$$K_{st} = \frac{800}{Re} + K_t \tag{2.9}$$

where, Re = pore Reynolds number = qd/ν in which ν = kinematic viscosity of fluid, and K_t = parameter to account for the angularity of the particles, ranging from 1 for polished spheres to 4 for rough and angular crushed stone.

Another widely used form of Izbash flow equation is based on experimental work done in a large packed-column by Wilkins (Bari and Hansen, 2002). He proposed the following dimensionally unbalanced equation for flow through coarse porous media:

$$V = Wm^{0.50} I^{0.54} \tag{2.10}$$

where W = Wilkins' constant (=52.43 for q in cm/s and m in cm) and m = hydraulic mean radius of the coarse porous media.

The product $Wm^{0.50}$ in Equation (2.10) is analogous to the geometric permeability of the porous media. The exponent 0.54 indicates that this equation is suited to the flow regime of nearly fully developed turbulence (Bari and Hansen, 2002).

Knowing that $V = q/n$, Equation (2.10) can be shown as:

$$I = \frac{1}{m^{0.93}} \left(\frac{q}{Wn} \right)^{1.85} \tag{2.11}$$

In the above equation, the term $1/m^{0.93}(Wn)^{1.85}$ represents parameter C in general power law [Equation (2.7)] and regarding the same equation N is replaced with 1.85.

For the quadratic type of non-Darcian flow law, Forchheimer (1901) proposed a two-term, nonlinear model for the hydraulic gradient in the underground as following;

$$I = A_1 q + A_2 q^2 \tag{2.12}$$

where $I = -dh/dx$ = hydraulic gradient; $h = z + P/\gamma$ = piezometric (hydraulic) head; P/γ = pressure head; A_1 and A_2 = empirically or theoretically determined constants.

Replacing hydraulic gradient, I, with $-dh/dx$, the Forchheimer equation takes the form:

$$-\frac{dh}{dx} = A_1 q + A_2 q^2 \tag{2.13}$$

Obviously, when A_2 equals to zero "0", both Equation (2.12) and (2.13) become identical with Darcy's law:

$$q = -\frac{1}{A_1}\frac{dh}{dx} \tag{2.14}$$

Since Equation (2.14) expresses Darcy's linear model, it can be concluded by equating it with Equation (2.4) that A_1 is the reciprocal of the hydraulic conductivity, K.

$$A_1 = \frac{1}{K} \tag{2.15}$$

or

$$K = \frac{1}{A_1} \tag{2.16}$$

Basak (1976) has presented the reported values for Forchheimer parameters A_1 and A_2 for sand and gravel. Bordier and Zimmer (2000) also tabulated Forchheimer parameters for gravel, geonet and geo-composite materials. Furthermore, in Venkatamaran and Rao (1998) the published data on the properties of porous media, which are particle size, porosity, intrinsic geometric permeability and the parameter for nonlinear term, A_2, was summarized.

In the same study (Venkatamaran and Rao, 1998) it was iterated that the linear parameter, A_1, depends upon the fluid properties and geometric permeability, k, on the other hand, the non-linear parameter A_2 is dependent upon the media properties such as size and shape of the media and porosity. They summarized the published data on properties of porous media.

Besides the relations mentioned above, Ward (1964) is one of those who successfully used a dimensional argument and proposed the following equation for the version of Forchheimer relation;

$$I = \left\{ \frac{\nu}{gk} \right\} q + \left\{ \frac{c}{g\sqrt{k}} \right\} q^2 \tag{2.17}$$

In the absence of the term, $\left\{ c / g\sqrt{k} \right\}$ Equation (2.17) becomes equivalent to Darcy's law. In addition, Ward (1964) experimentally obtained a value of c = 0.55 for the transition range between laminar and turbulent flows.

2.4 Governing Equations

2.4.1 Energy Equation

In this thesis, focus is placed on ordinary flow conditions, where the flow takes place only through the rubble mound weir. The flow over the weir is excluded in this work. Model parameters and cross section details are given in both Figure 2.1 and Figure 2.2.

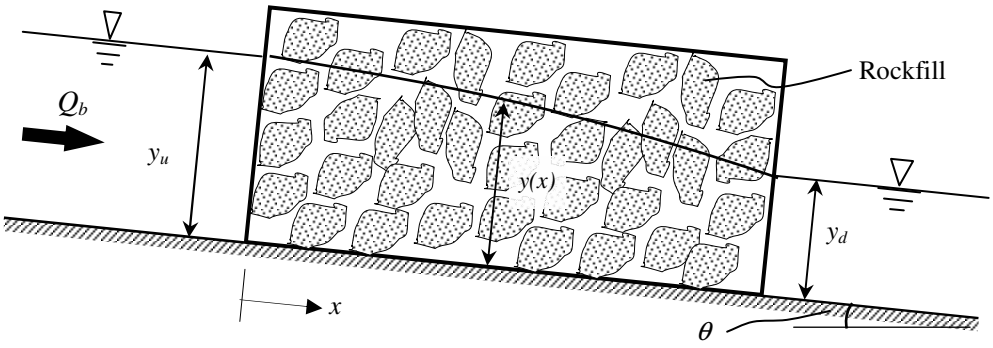

Figure 2.1 Model system and definition of variables

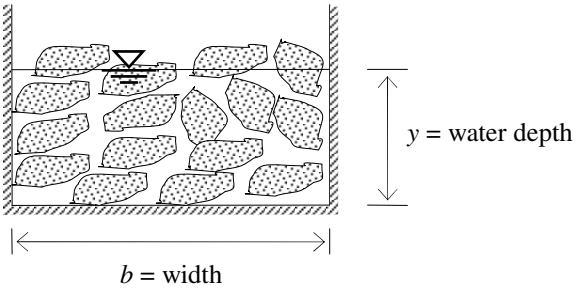

Figure 2.2 Cross sectional view of model system

The flow in such cases behaves in a manner that is similar in some ways to open channel flow. However, the longitudinal variation in water depth is no longer partly governed by the roughness of the streambed, as in the case for open channel flow, but by the characteristics of the coarse porous media, which now fills the formerly open channel.

In the study of Bari and Hansen (2002), calculation of water surface profiles for gradually varied flow was done by using Wilkins and Stephenson's equations. In that work, the 1-D dynamic equation of flow through porous medium under steady-state conditions was shown to be:

$$\frac{dy}{dx} = \frac{S_0 - S_f}{1 - Fr_p{}^2} \tag{2.18a}$$

$$\frac{dy}{dx} = f(x, y) \tag{2.18b}$$

where, x = longitudinal coordinate originated at upstream boundary of weir; y = vertical water depth = $y_p \cos\theta$; y_p = piezometric water depth; θ = stream bed angle (degree) ; S_0 = bed slope of channel = $\sin\theta$; S_f = friction slope; Fr_p = pore Froude number = $q/\sqrt{gD}$; D = hydraulic depth = A/T , in which T is the top width.

For non-Darcian flow through buried streams, S_f is evaluated using Stephenson and Wilkins' equations. The numeric solutions were obtained by replacing S_f with hydraulic gradient I in the work of Bari and Hansen (2002) with the application of procedure used by Prasad (1970). Governing equations were obtained with substituting Stephenson and Wilkins' equations [Equations (2.8) and (2.11)] into Equation (2.18a) and following equations arise:

$$\frac{dy}{dx} = \frac{S_0 - \frac{K_{st}}{gd} q^2}{1 - Fr_p{}^2} \tag{2.19}$$

$$\frac{dy}{dx} = \frac{S_0 - \frac{1}{m^{0.93}} \left(\frac{q}{Wn} \right)^{1.85}}{1 - Fr_p{}^2} \tag{2.20}$$

In this study, unlike the previous works, flow is modeled with the usage of Ward formulation (Ward, 1964) given by Equation (2.17). Thence, in the analysis of non-Darcian flow through weir Forchheimer equation was used like the study of Michioki et al. (2005). This differential equation was solved by numerical method similar to the one in Bari and Hansen (2002).

For the model given in Figure 2.1 and 2.2 it is considered that gradient of the total energy loss, dH/dx is balanced by the hydraulic gradient I given by Forchheimer equation (Michioki et al., 2005). The relationship is then written as follows:

$$\frac{d}{dx}\left(\frac{V^2}{2g}\right) + \frac{dy}{dx} - S_0 + \left\{\frac{\nu}{gk}\right\} q + \left\{\frac{c}{g\sqrt{k}}\right\} q^2 = 0 \tag{2.21}$$

where, $H = V^2/2g + y + z$ = total head; z = channel bed elevation; V= average fluid velocity = q/n .

Equation (2.21) can be rearranged to obtain change of water depth along distance as follows;

$$\frac{dy}{dx} = \frac{S_0 - \left\{\left(\frac{\nu}{gk}\right)\frac{Q_b}{y}\right\} - \left\{\left(\frac{c}{g\sqrt{k}}\right)\frac{Q_b^{\,2}}{y^2}\right\}}{1 - \left\{\frac{1}{n^2}\left(\frac{Q_b^{\,2}}{gy^3}\right)\right\}} \tag{2.22}$$

2.5 Concluding Remarks

In this chapter, a detailed literature survey is provided. According to this literature investigation, necessity for the investigation of problem considered in this thesis is pointed out. For the solution of the problem, necessary background information is summarized. This covers Darcy and non-Darcian flow equations. Moreover, the conceptual model of the problem is given in Figure 2.1 and Figure 2.2. Finally, obtained governing equations are explained.

CHAPTER 3

NUMERICAL SOLUTION OF THE PROBLEM

This chapter starts with the summary of necessity of numerical solution. Then, numerical solution to the governing equations given in previous chapter is explained in detail. Afterwards, procedure used solving the governing equations are given.

3.1 Introduction

Solving a mathematical groundwater model requires calculating the values of head at each point in the system. The reliability of predictions using a groundwater model depends on how well the model approximates the field situation. Using governing equations it is possible to write an expression for head as a function of the space coordinates. Generally, this expression is a partial differential equation with appropriate initial and boundary conditions.

Partial differential equations describe a certain physical phenomenon at a point in a domain. In most cases, the dependent variables are variables for which solution is required, such as, piezometric head, pressure, specific discharge etc. In addition, the independent variables are spatial variables (x, y, z) and time (t). Generally, partial differential equations can be called as mathematical models of actual phenomena.

In many cases, the partial differential equations cannot be solved by exact analytical methods. This is especially so when the equations are too complex, the domain is inhomogeneous, analytical solution is very difficult to apply to a specific problem or the assumptions to obtain an analytical solution may not be realistic. In those cases, numerical methods are used. Numerical solutions yield approximate values for only a predetermined, finite number of points in the problem domain.

3.2 Water Surface Profile Analysis

For flow through porous media that follows Darcy's law, the velocity is very small ($<10^{-2}$ m/s). Consequently, the kinetic energy of the flow can be negligible. This is not the case for non-Darcian flow. The flow in such cases behaves in a manner that is similar in some ways to open channel flow. Since unconfined gradually varied non-Darcy flow is analogous to that of open channels, it was hypothesized that flow profiles for the former could be computed in the same general manner as is done for the latter.

Several investigators have presented methods of integration of the equation of gradually varied flow. In almost all the methods, hydraulic exponents or some form of varied flow function or both have been used to render the equation more tractable for solution. Chow presented a method of integration in which a set of tables of the varied flow function is required (Prasad, 1970). Keifer and Chu, as stated by Prasad (1970), have presented a method of numerical integration primarily for circular conduits. Later, Pickard (1963) presented a numerical integration based on a finite series of polylogarithms and polynomials as implied in the Chow method. There are several other methods of flow profile computation. However, no single has been found to be suitable for all applications (Prasad, 1970).

In literature, mostly two procedures were used for computing steady Gradually-Varied Flow (GVF) profiles. They are the method of integration used by Prasad (1970) and the Standard Step Method (SSM) (Chow, 1959). The method proposed by Prasad numerically integrates the one-dimensional dynamic equation for open channel flow [the differential equation analogous to Equation (2.18)] at successive cross-sections, starting at a known water level. Under this method, the direction of computation does not depend on whether the flow is subcritical or supercritical. On the other hand, the SSM applies the energy equation successively across pairs of cross-sections where the depth at one of them is known. For this method, the direction of computation must be upstream for subcritical flow, and downstream for supercritical flow.

In this study, only first computational scheme used by Prasad was modified and used for simulation of non-Darcian water surface profiles for flow through porous media. Moreover, while computing the water surface profiles, trapezoidal method of integration is used to solve partial differential equation [Equation (2.18)]. The details of this method are explained in the following section.

3.2.1 Trapezoidal Method of Integration

Stephenson (1979) hypothesized that ordinary open channel flow and flow through rockfills are analogous, implying that steady water surface profiles for the latter can be computed by integration of Equation (2.18a). The differential equation of gradually varied flow is nonlinear because parameters in the right-hand side of the equation depend on water head elevations. Equation (2.18a) may be integrated by analytical, graphical, or numerical methods. However, the analytical integration of Equation (2.18a) would have been impractical even impossible. Using the techniques of numerical analysis, the problem of accuracy and convergence affecting the solution can be kept under proper control.

An iterative method of numerical integration of Equation (2.18a) will be described which may be used to integrate any first order linear or nonlinear differential equation.

$$y_{i+1} = y_i + \Delta y \tag{3.1}$$

or

$$y_{i+1} = y_i + \frac{dy}{dx}\Delta x \tag{3.2}$$

Since a closed-formed integration is not generally possible, it is necessary to resort to numerical integration. This requires evaluation of dy/dx, which is equal to the function $f(x, y)$ in Equation (2.18b) at a number of discrete points x_i and so as to obtain solutions y_i at these points, where $i = 1, 2, 3, ..., M$ (M being the total number of cross-sections in the reach being considered).

If the values of the function *f(x, y)* are plotted as a function of the variable *x*, the curve shown in Figure 3.1 will be obtained. The area between sections x_i and x_{i+1} will give the difference between y_i and y_{i+1}. The solution at one cross-section is used to generate the solution at the next cross-section in the simplest numerical integration methods, as long as a suitable boundary conditions of the form $y = y_u$ at $x = x_u$ are available. That means it integrates the one-dimensional dynamic equation for open channel flow at successive cross-sections, starting at a known water level. Adopting this general method, Equation (3.1) and Equation (3.2) can be written as:

$$y_{i+1} = y_i + \int_{x_i}^{x_{i+1}} f(x, y)dx \tag{3.3}$$

If the function *f(x,y)* varies linearly, the above equation can be rewritten for the scheme of the trapezoidal method while $\dot{y}$ representing the simple derivative $\dot{y} = dy/dx$.

$$y_{i+1} = y_i + \frac{\dot{y}_{i+1} + \dot{y}_i}{2}\Delta x \tag{3.4}$$

or

$$y_{i+1} = y_i + \frac{\Delta x_i}{2}\left\{\left(\frac{dy}{dx}\right)_i + \left(\frac{dy}{dx}\right)_{i+1}\right\} \tag{3.5}$$

Equation (3.4) and Equation (3.5) can be used in computation of the elevation of section x_{i+1}. The schematic view of trapezoidal method of integration of function *f(x,y)* is given in Figure 3.1.

In almost all the other methods of flow profile computation, the type of flow profile has to be determined or assumed before the solution can proceed. In the proposed method, only the starting depth and the desired direction (upstream or downstream) of computation are needed. This is so because the differential equation of gradually varied flow needs only one initial condition y_u for the solution; all other details of the profile are automatically fixed for a given channel and given discharge, *Q*.

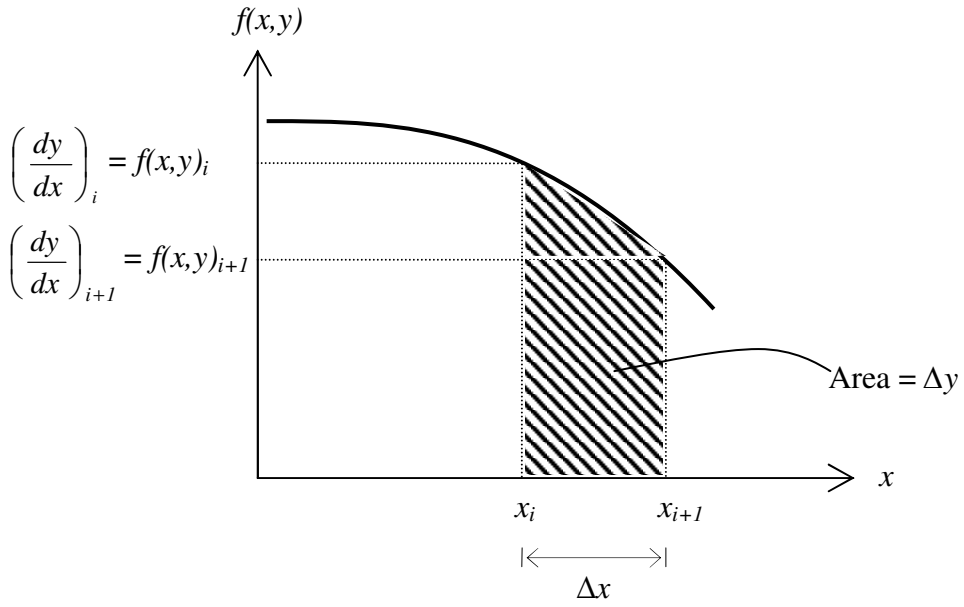

Figure 3.1 Trapezoidal method of integration

3.2.2 Non-Darcian Flow Profile Modeling By Iteration

In the analysis, the model weir on the longitudinal cross-section is assumed to have a rectangular shape for analytical simplicity, whereas a prototype weir requires a trapezoidal geometry with slopes on the upstream and downstream faces for dynamic stability. The flow is one-dimensional and the flow region is divided into the three regions, as shown in Figure 3.2.

The first region ends at the cross section at $x=0$ where flow suddenly converges from the open channel to the porous body. The second one is the reach between $x=0$ and $x=L$ in which the subsurface flow is gradually varied in the porous body. The third and final region starts at the cross section at the downstream end of the weir, $x=L$, where flow rapidly diverges from the porous body to the open channel.

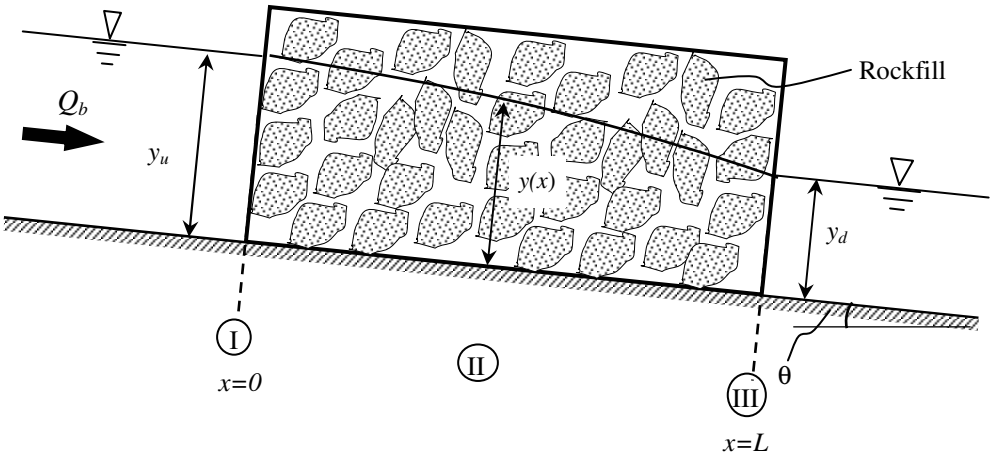

Figure 3.2 Definition of weir model regions

Compared to the rapid flow transition around $x=0$, the longitudinal variation of flow in the second region is rather gradual. In this thesis, Equation (2.17) is applied to describe the flow resistance in the rockfill structure, where the apparent velocity or the superficial velocity is defined as Darcy velocity by the equation $q = Q/A$.

As mentioned in section 2.4.1 in Chapter 2, the longitudinal variation in water depth is no longer partly governed by the roughness of the streambed, as in the case for open channel flow, but by the characteristics of the coarse porous media, which now fills the formerly open channel. Using this definition, the one-dimensional dynamic equation of flow through rockfills under steady-state conditions can be shown as Equation (2.18). This equation is analogous to the equation applicable to open channels for which the term Fr_p is replaced by the Froude number Fr associated with ordinary open channel flow, and the friction slope S_f is computed using a uniform-flow resistance equation (such as the Manning equation). For non-Darcian flow through porous medium, S_f is evaluated using a non-Darcian flow equation. It is worthwhile mentioning that for most open channels $\theta \leq 4°$ and in such cases the distinction between y and y_p is so insignificant that it is common

practice to assume that $dy/dx = dy_P/dx$.

For the porous medium in this thesis, it is considered that gradient of the total energy loss, $d\{(V^2/2g)+P/\gamma+z\}/dx$ is balanced by the hydraulic gradient *I* given by Forchheimer equation. Then, the relationship is written as Equation (2.21) and Equation (2.22).

When dy/dx expression in Equation (3.5) is replaced with the one given by Equation (2.18a), following relation is obtained.

$$y_{i+1} = y_i + \frac{\Delta x_i}{2}\left\{\left(\frac{S_0(x)-S_f(x,y)}{1-Fr_P{}^2(y)}\right)_i + \left(\frac{S_0(x)-S_f(x,y)}{1-Fr_P{}^2(y)}\right)_{i+1}\right\} \tag{3.6}$$

In previous studies, such as Bari and Hansen (2002), S_f was evaluated by using Stephenson and Wilkins equations [Equation (2.8) and Equation (2.11) respectively]. Therefore, inserting these equations into Equation (3.6), the following equations are obtained:

$$y_{i+1} = y_i + \frac{\Delta x_i}{2}\left\{\left(\frac{S_0-\frac{K_{st}}{gd}q^2}{1-Fr_p{}^2}\right)_i + \left(\frac{S_0-\frac{K_{st}}{gd}q^2}{1-Fr_p{}^2}\right)_{i+1}\right\} \tag{3.7}$$

$$y_{i+1} = y_i + \frac{\Delta x_i}{2}\left\{\left(\frac{S_0-\frac{1}{m^{0.93}}\left(\frac{q}{Wn}\right)^{1.85}}{1-Fr_p{}^2}\right)_i + \left(\frac{S_0-\frac{1}{m^{0.93}}\left(\frac{q}{Wn}\right)^{1.85}}{1-Fr_p{}^2}\right)_{i+1}\right\} \tag{3.8}$$

Contrary to these previous works, in this thesis, S_f is evaluated by using Forchheimer equation. Inserting Equation (2.17) into Equation (3.6) yields the following relation.

$$y_{i+1} = y_i + \frac{\Delta x_i}{2}\left\{\left(\frac{S_0 - \left\{\left(\frac{\nu}{gk}\right)\frac{Q_b}{y}\right\} - \left\{\left(\frac{c}{g\sqrt{k}}\right)\frac{Q_b^{\,2}}{y^2}\right\}}{1 - \left\{\frac{1}{n^2}\left(\frac{Q_b^{\,2}}{gy^3}\right)\right\}}\right)_i + \left(\frac{S_0 - \left\{\left(\frac{\nu}{gk}\right)\frac{Q_b}{y}\right\} - \left\{\left(\frac{c}{g\sqrt{k}}\right)\frac{Q_b^{\,2}}{y^2}\right\}}{1 - \left\{\frac{1}{n^2}\left(\frac{Q_b^{\,2}}{gy^3}\right)\right\}}\right)_{i+1}\right\} \tag{3.9}$$

The above equation is the main equation of this thesis approach.

As mentioned before, the procedure for computing water surface profile is similar to the one used by Prasad (1970). Computing water surface profile needs solving Equation (3.9). However, this equation is non-linear and calculation should be done by iterative method. The computation process is provided by the flow chart shown in Figure 3.3 and step-by-step explanation is given below.

Step 1. Start. Rockfill parameters, k, K, n; channel and fluid properties, S_0, Q_b, ν, g; identification of constants, c; and initial water depth y_u are inserted.

Step 2. Start iteration from known water depth y_i

Step 3. Calculate $(dy/dx)_i$ using Equation (2.22);

Step 4. Assume $(dy/dx)_{i+1} = (dy/dx)_i$;

Step 5. Calculate y_{i+1}^{j} using Equation (3.5);

Step 6. Calculate $(dy/dx)_{i+1}^{j}$ using y_{i+1}^{j} ;

Step 7. Calculate y_{i+1}^{j+1} using Equation (3.9);

Step 8. Check $\varepsilon = \left| \frac{y_{i+1}^{j+1} - y_{i+1}^{j}}{y_{i+1}^{j}} \right| \leq 10^{-7}$;

Step 9. If not, go to *Step 6* with assuming $y_{i+1}^{j} = y_{i+1}^{j+1}$;

yes, stop iteration;

Step 10. Result, $y_{i+1} = y_{i+1}^{j+1}$

Step 11. Check if $y_{i+1} = y_M$; not go to *Step 2* with assuming $y_i = y_{i+1}$;

otherwise, STOP.

In the procedure explained above, superscript *j* refers to the iteration level.

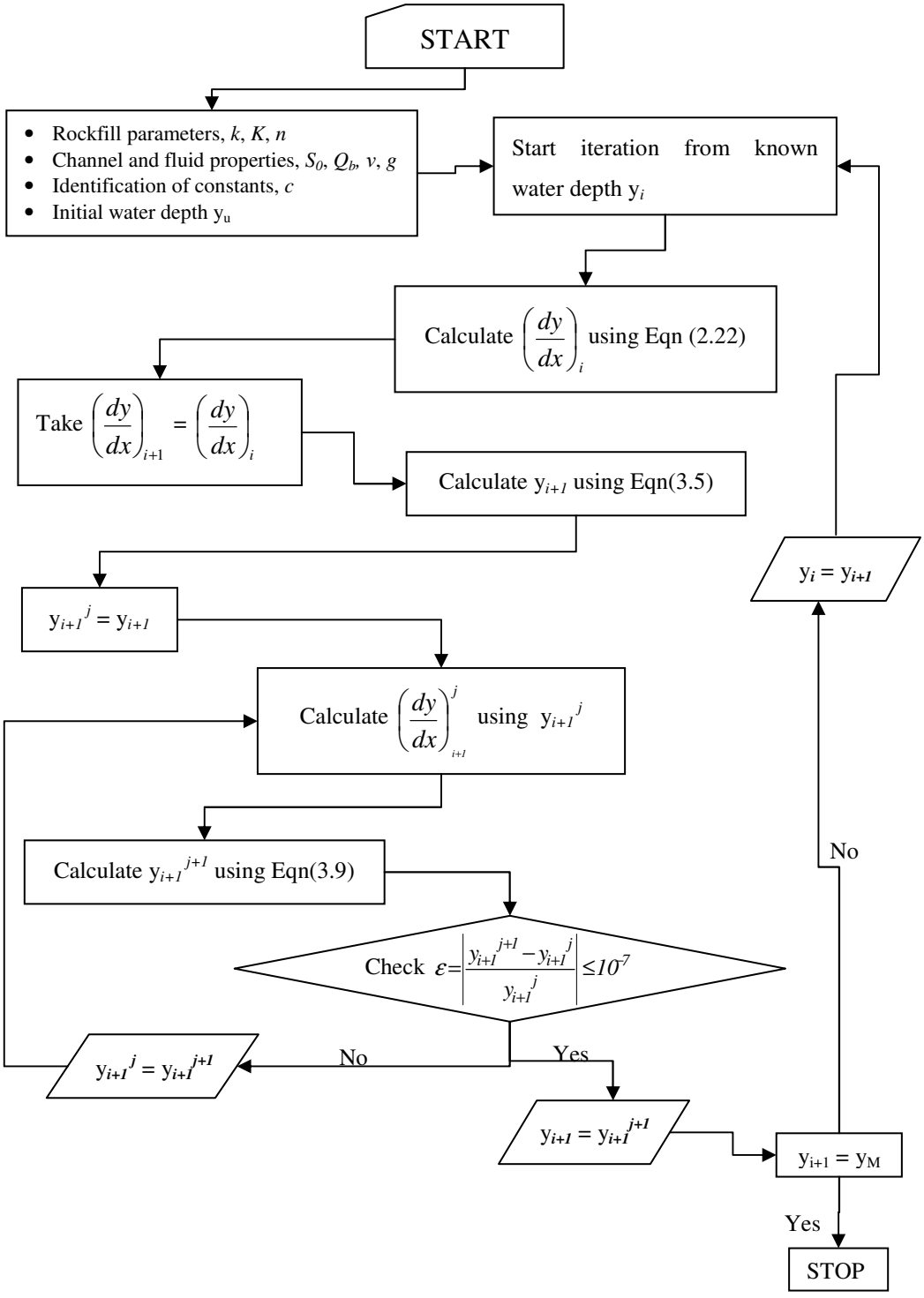

Figure 3.3 Flow chart used in computation of water surface profile

In order to compare water surface profiles with previous studies in the literature, Equation (3.7) and Equation (3.8) are solved by similar procedure explained above. Both Wilkins' equation and the Stephenson equations are used as the basis for friction slope (S_f) determination. Flow charts and step-by-step explanations of these two approaches are given in Appendix A. The assumptions are the same as those used in the solution made by applying Forchheimer relation to gradually varied flow for flow through rockfills. Comparison of the water surface profiles computed by three methods (Forchheimer, Stephenson, and Wilkins) is given in Chapter 5.

3.3 Concluding Remarks

In this chapter, need for numerical solution for water surface profile computation is explained in detail. Available methods of integration for gradually varied flow in literature are briefly reviewed. For practical reasons, trapezoidal method of integration is chosen. The brief information of this method is given. The essential equation of proposed numerical integration in this thesis approach is also identified in this chapter. After that, the procedure of numerical integration for the non-Darcian flow profile is explained step by step.

CHAPTER 4

EXPERIMENTAL INVESTIGATION

This chapter explains the experimental investigation of the physical weir model in the laboratory. First of all, experimental setup is explained in detail. Then, measurements of all data (water head elevations and discharge) are shown. After that, type of experiments and experimental conditions are described.

4.1 Experimental Setup

Physical model tests evaluate the performance of the mathematical developments. Therefore, in this study laboratory experiments are carried out to verify the numerical solution of the governing equation obtained by using Forchheimer relation as explained in Chapter 3. Tests are carried out at the Hydromechanics Laboratory of Middle East Technical University. In the experiments, the flume shown schematically in Figure 4.1 is used. The flume is 7.54 m long, 0.675 m wide, 0.575 m deep. The channel is horizontal and equipped with a flap gate installed at the downstream end of the channel to control the tailwater conditions.

Bricks having the dimensions of 22.5 cm x 10.5 cm x 6.0 cm are used as weir material. Bricks are chosen as a weir material because they were readily available in laboratory. This is economical and leads time gaining. Arrangement of the bricks are given in Figure B.2 in Appendix B. The weir model constructed from bricks has dimensions 2.106 m long, 0.675 m wide, and 0.500 m deep. The weir model is rectangular with vertical upstream and downstream faces.

All measurements of water surface profile are conducted from sidewall of the channel. The arrangement of measuring points is shown in Figure 4.2. The photograph of the experimental setup is shown in Figure 4.3. Moreover, additional photographs of other view of the experimental setup are given in Appendix B.

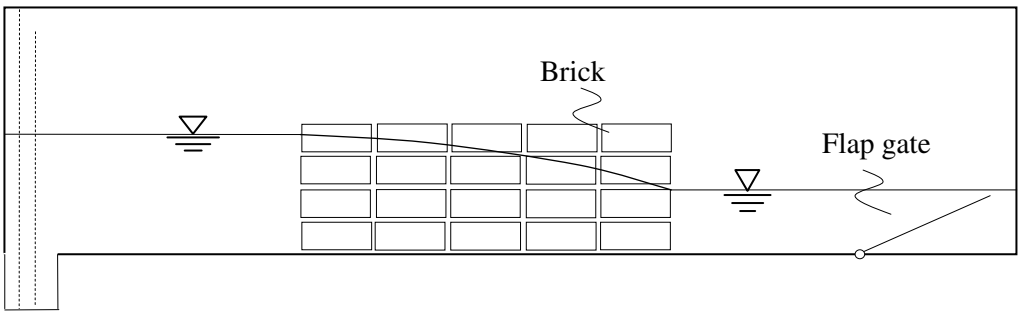

Figure 4.1 The schema of side view of the flume used in experimental studies.

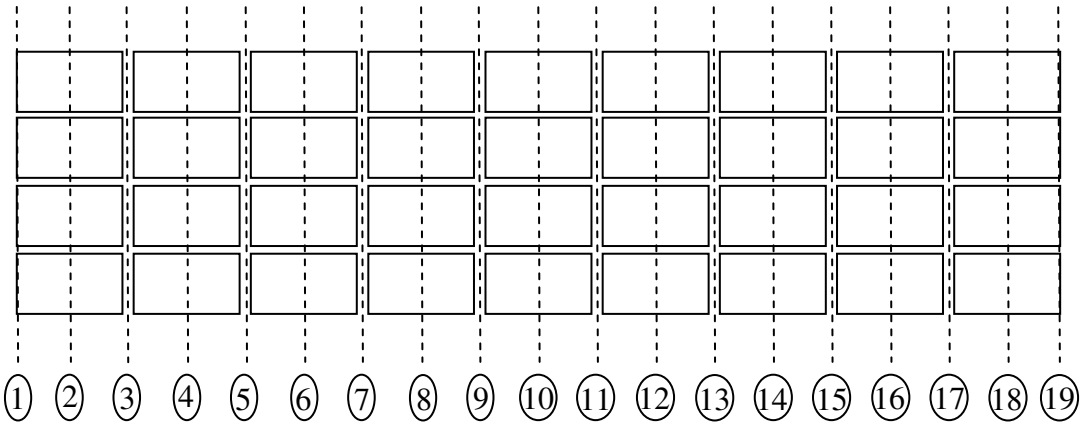

Figure 4.2 Side schematic view of the arrangement of measuring points

Figure 4.3 Photograph of the experimental setup

4.2 Discharge Measurement

A sharp crested rectangular weir made of fiberglass is used in the determination of flowrate. For this purpose, the head over the crest is measured by a point gage (Figure 4.4). The discharge is computed, as it is done in Yılmaz (2003), from the equation (Henderson, 1966):

$$Q = C_d \frac{2}{3}\sqrt{2g} L_l Z^{3/2} \tag{4.1}$$

where Q is discharge, C_d is the discharge coefficient, L_l is the effective length of the crest and Z is the measured water head over the crest, excluding the velocity head. The discharge coefficient, C_d, in Equation (4.1) is determined by the equation given by Rehbock in 1929. (Addison, 1954 and King, 1954):

$$C_d = 0.605 + \frac{1}{1000Z} + 0.08\frac{Z}{P'} \tag{4.2}$$

where P' is the weir height.

Figure 4.4 Photograph of the point gage used in discharge measurement

4.3 Experiments

For weir flow, five possible flow patterns can be observed (Maeno et al., 2002). As shown in Figure 4.5, they are non-overflow, non-overflow limit, transition state, overflow limit and overflow. Non-overflow is the state that the water flows only through the rockfill weir, and non-overflow limit is the state that the free surface disappears from the upper edge of the weir crest. In addition, transition flow is the state that the flow gets into the rockfill over the weir. Overflow limit is the flow profile that the free surface reaches just the downstream edge of the weir crest. In measurements and calculations, only non-overflow and non-overflow limit patterns are taken into consideration in this thesis. These two flow conditions are related with only flow through weir and they can be referred as porous medium flow. Regarding these flow conditions, two groups of experiments are conducted.

The first group experiments are done for the determination of hydraulic conductivity of the porous medium. In order to achieve this aim, Darcy law should be valid. That means obtained water surface profiles must be linear. Hence, all flow conditions in this group are arranged to obtain Darcy flow through porous medium. On the other hand, in the second group, the objective is to obtain non-Darcian flow through the weir. Non-linear flow profiles should be obtained experimentally. Then, the measured results could be used to compare with the results of numerical analysis, which uses the computational method explained in the water surface profile analysis part in Chapter 3. In order to verify the types of flows Reynolds numbers presented in Table 4.1 are used. For Darcy flow case Reynolds number is between 1-10, and for non-Darcian this number is higher than 10.

Table 4.1 Determination of flow types according to Reynolds number

Flow type	**Exp no**	**y_u**	**y_d**	**Q**	**Re_u**	**Re_d**
Darcian	1	0.350	0.311	0.00101	7.4	8.3
	2	0.370	0.335	0.00097	6.7	7.4
	3	0.375	0.350	0.00092	6.3	6.8
Non-Darcian	4	0.421	0.213	0.00438	26.7	52.8
	5	0.480	0.350	0.00384	20.6	28.2
	6	0.403	0.083	0.00438	27.9	135.6
	7	0.400	0.083	0.00425	27.3	131.6
	8	0.316	0.190	0.00195	15.9	26.4
	9	0.320	0.210	0.00174	14.0	21.3
	10	0.443	0.335	0.00308	17.9	23.6
	11	0.425	0.330	0.00308	18.6	24.0
	12	0.430	0.338	0.00308	18.4	23.4
	13	0.386	0.310	0.00216	14.4	17.9

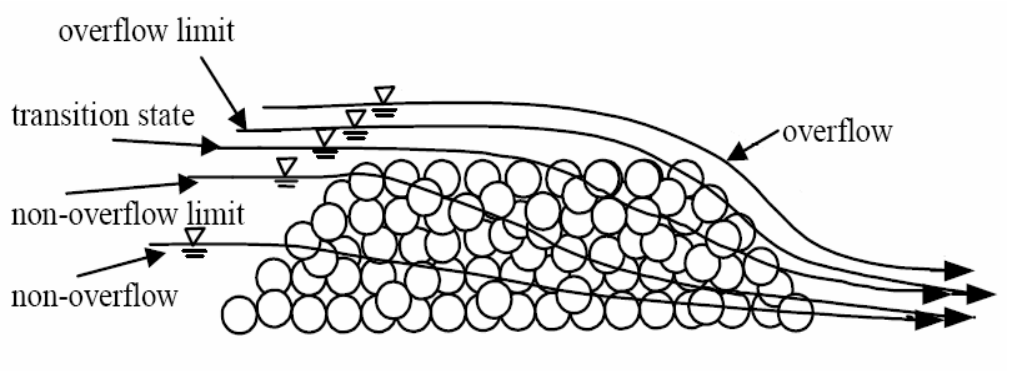

Figure 4.5 Possible flow patterns (Maeno et al., 2002)

4.3.1 Determination of Hydraulic Conductivity

Hydraulic conductivity, *K*, describes how easy a geologic medium can transmit groundwater, and is one of the fundamental parameters for investigating groundwater movement. Values of *K* for saturated groundwater flow can be measured from a variety of methods, such as grain size analysis, permeameter tests, slug tests, pumping tests, flow meter tests, and geophysical methods (Qian et al., 2007).

A very brief review of the literature used in the development of the hydraulic conductivity expressions is presented in the study carried by Hannoura and McCorquadale (1985). An extensive and well-documented study of the hydraulic conductivity of crushed rock had been presented by Dudgeon (1966). He used ungraded material with median diameters varying from 0.5 – 110 mm, however he did not present a general equation for his results. Other authors, such as Ward (1964), Ahmed and Sunada (1969), Engelund (1953), and Kovacs (1969) had published other important contributions (Hannoura and McCorquodale, 1985).

In addition, a number of non-Darcian flow investigations had been carried out. These studies involved one- and two-dimensional flows, one and two phase flows, and steady and unsteady conditions. In those studies, graded river gravel and crushed rock in various sizes were used. The work of Ward (1964), and Ahmed and

Sunada (1969) was extended by Arbhabhirama and Dinoy (1973) in order to develop a moody diagram type presentation for the friction coefficient. Later, applying that approach to a wide range of flow conditions showed that it is not statistically reliable (Hannoura and McCorquodale, 1985).

According to the literature survey mentioned above, there is no general equation for determination of hydraulic conductivity. Therefore, in this thesis Darcy flow type of experiments are carried out to obtain a realistic and reliable hydraulic conductivity of the weir model used in all experiments similar to the previous thesis (Banna, 1997; Polatel, 2000; and Korkmaz, 2002).

For one-dimensional and steady Darcy flow, governing differential equation is as follows,

$$\frac{d^2h^2}{dx^2} = 0 \qquad \text{for } 0 \le x \le L \tag{4.3}$$

where h is piezometric head.

Integration of the above equation yields the following analytical solution;

$$h^2 = c_1 x + c_2 \tag{4.4}$$

where c_1 and c_2 are constants of integration.

Boundary conditions are;

$$h_0 = h_u \qquad \text{at } x = 0 \tag{4.5}$$

$$h_L = h_d \qquad \text{at } x = L \tag{4.6}$$

Using these boundary conditions, c_1 and c_2 may be determined. After inserting values of c_1 and c_2 into Equation (4.4), analytical solution for the water table elevation of the flow become as in Equation (4.7).

$$h^2 = \frac{h_u^{\,2} - h_d^{\,2}}{L} x + h_u^{\,2} \tag{4.7}$$

In addition, discharge at any section located at a distance x from the origin can be calculated by differentiating Equation (4.7) and from the Darcy's law [Equation (2.7)]. The result is the following expression;

$$Q_b = K\frac{h_u{}^2 - h_d{}^2}{2L} \tag{4.8}$$

or

$$K = \frac{2Q_bL}{(h_u{}^2 - h_d{}^2)} \tag{4.9}$$

After combining Equation (4.7) and Equation (4.8), following relation is obtained.

$$h^2 = \frac{2Q_b}{K}x + h_u{}^2 \tag{4.10}$$

Both Equations (4.7) and (4.10) may be put into the following common form:

$$h^2 = mx + h_u{}^2 \tag{4.11}$$

As a result, Equation (4.11) gives a straight line when h^2 is plotted against x on an arithmetic scale. Consequently, the slope of this line can be used to determine the hydraulic conductivity, K, from laboratory measurements. Equation (4.10) indicates that the slope, m, is given by

$$m = \frac{2Q_b}{K} \tag{4.12}$$

or

$$K = \frac{2Q_b}{m} \tag{4.13}$$

The slope m may be determined in two ways:

a) Using Equation (4.7);

$$m_1 = \frac{h_u{}^2 - h_d{}^2}{L} \tag{4.14}$$

The slope m_1 is obtained with the help of experimentally obtained h_u, h_d, and L.

b) Using least square curve fitting to the straight-line h^2 versus x (m_2). For this purpose Excel program may be used for two experimental data as shown in Figure 4.6.

The value of hydraulic conductivity, K, may now be calculated from Equation (4.13), using these two slopes, provided that Q_b is also known from experimental measurements.

Procedure for conducting experiments and analysis of data is given below.

Step 1. Constant head elevations at upstream (h_u) and downstream (h_d) are set to two different values, in such a way that the difference between them is sufficiently small to create Darcy flow.

Step 2. After the flow reaches the steady state conditions, the values of water surface profile measurements through h_u to h_d and also discharge, Q, are recorded as mentioned in experimental setup and discharge measurement sections.

Step 3. *Steps 1* and *2* are repeated for different values of ($h_d - h_u$). In the present study, two sets of experiments are conducted for Darcy flow analysis. The data related to these experiments are given in Table 4.1 and Table 4.2.

Step 4. For each set of data h^2 versus x graph are plotted and shown in Figure 4.6.

Step 5. Two best-fit lines are calculated for the set of experimental data with the help of excel program trendline tool. Equations of these graphs are shown in Figure 4.6.

Step 6. From the slopes of these two lines, m_{21} and m_{22} constants are found by using equations shown in Figure 4.6 and given in Table 4.2.

Step 7. To check these m_2 values, m_1 values for each case are computed and stated in Table 4.2.

Step 8. Using Equation (4.13), for each experiment K_1 and K_2 values are calculated. These values are also given in Table 4.2. Since obtained values are slightly different form each other, the average of two K values are used for weir model and it is presented in Table 4.2.

After applying this procedure, the hydraulic conductivity of the weir model in the laboratory is taken as $K = 0.23374$ m/s, as the average of K values of two experimental data, $K_1 = 0.22989$ m/s and $K_2 = 0.23759$ m/s.

The first two experiments are conducted for determination of hydraulic conductivity that means it is an identification problem. This type of problem involves determining the parameters, which govern the response of the system with given inputs. Schematic view of this explanation is given in Figure 4.7(a).

Moreover, to check further the calculated hydraulic conductivity another experiment is conducted. This requires prediction of discharge and water head elevation with known geometry and properties of weir that means it is a prediction problem. Solving prediction problem means solving a model in order to obtain the future distribution of water levels or piezometric heads with known geometry and properties of weir. Schematic presentation is shown in Figure 4.7(b). Discharge is checked using Equation (4.8) and related calculations are given in Table 4.3. Water head elevations are checked and presented in Chapter 5.

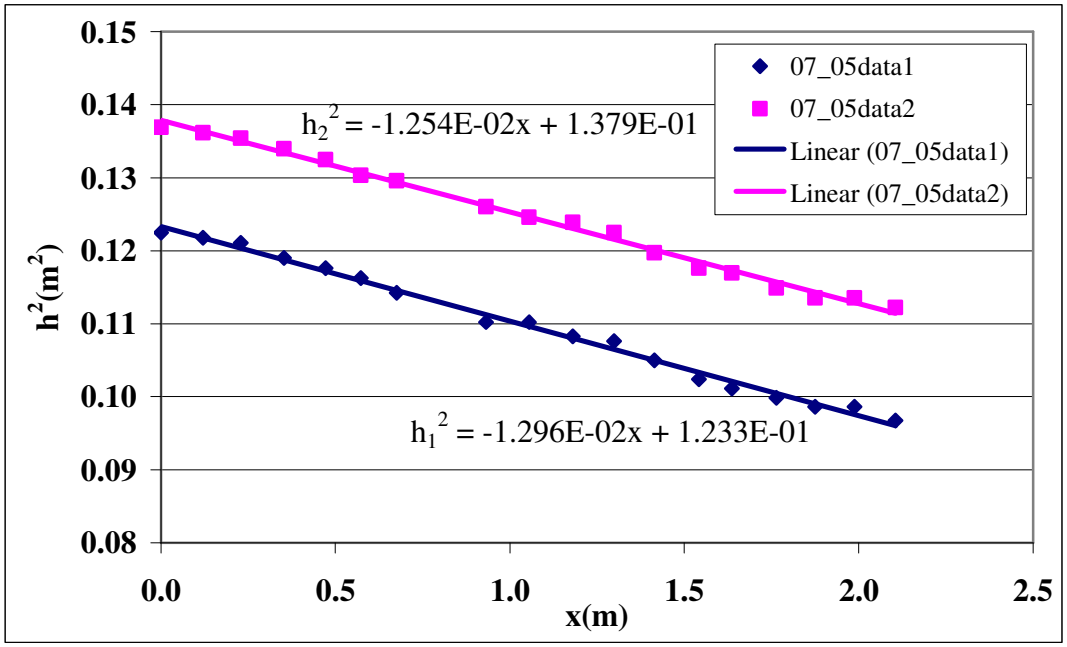

Figure 4.6 Graph of first type of experimental data

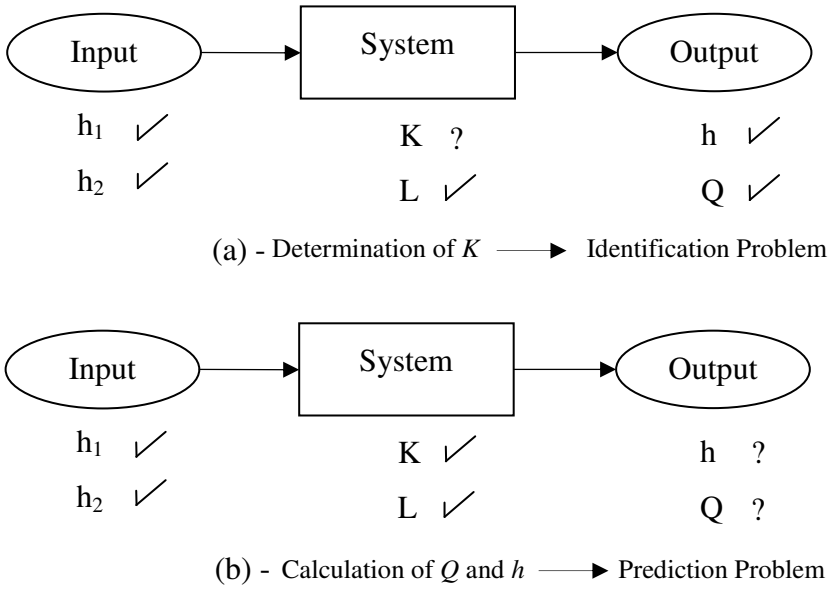

Figure 4.7 Schematic views of the problem types

Table 4.2 Water head elevation measurements for two experiments

Measuring points	***x*(cm)**	y_{exp1} **(cm)**	y_{exp2} **(cm)**
1	0.00	35.0	37.0
2	12.00	34.9	36.9
3	22.80	34.8	36.8
4	35.30	34.5	36.6
5	47.20	34.3	36.4
6	57.30	34.1	36.1
7	67.60	33.8	36.0
8	77.70	33.5	35.6
9	93.10	33.2	35.5
10	105.50	33.2	35.3
11	118.10	32.9	35.2
12	129.90	32.8	35.0
13	141.50	32.4	34.6
14	154.20	32.0	34.3
15	163.60	31.8	34.2
16	176.40	31.6	33.9
17	187.60	31.4	33.7
18	198.80	31.4	33.7
19	210.60	31.1	33.5

Table 4.3 Summary of hydraulic conductivity determination

Experiment No	**1**	**2**
Z **(m) =**	0.8	0.78
C_d **=**	0.732	0.735
Q **(m^3/s) =**	0.00101	0.00097
Q **(lt/s) =**	1.0055	0.9722
Q **(m^3/day) =**	86.878	84.001
y_1**-**y_2 **(cm)=**	3.9	3.5
m_1 **=**	0.01224	0.01172
m_2 **=**	0.01296	0.01254
K **(m/s) =**	0.22989	0.23759
$K_{average}$ **(m/s) =**	0.23374	

Table 4.4 Verification of hydraulic conductivity by discharge

Experiment No	**3**
***Z* (m) =**	0.75
C_d **=**	0.740
Q **(m^3/s) =**	**0.00092**
Q **(lt/s) =**	0.92298
Q **(m^3/day) =**	79.745
$y_1^2-y_2^2$ **=**	0.01813
$(y_1^2-y_2^2)/2L$ **=**	0.00430
$Q_{calculated}$ **(m^3/s)=**	**0.00101**

4.3.2 Non-Darcian Flow Profile

After conductivity experiments, to find the water surface profiles for non-Darcian type of flow through porous media, another set of experiments are conducted. Measurements of experimental data are explained in experimental setup, discharge measurement, and experiments part of this chapter. In all these experiments, porosity of the weir remains the same. Calculation of the porosity of the weir is given in Table 4.4. All the measurements of water surface profile are conducted from the sidewall of the channel. The arrangement of measuring points is shown in Figure 4.2. Discharge is measured by means of a sharp crested rectangular weir shown in Figure 4.4.

In these sets of experiments, flow is turbulent according to its Reynolds number that means it does not obey the Darcy's law. These experiments are carried out to verify the numerical modeling explained in Chapter 3. While conducting experiments in order to make sure that steady state conditions are achieved, the water levels and discharge are measured with 15 minutes of intervals without changing any condition. When there is no change between the last two successive checks, the water surface profile is taken as experimental data.

An example of water surface profile conducted in this group of experiments is given in Figure 4.8 and related data is given in Table 4.5. In order to ease the reading of the text, all the other profiles and related data are presented in Appendix A. Moreover, all the results of these experiments and comparisons with numerical solution are given in Chapter 5.

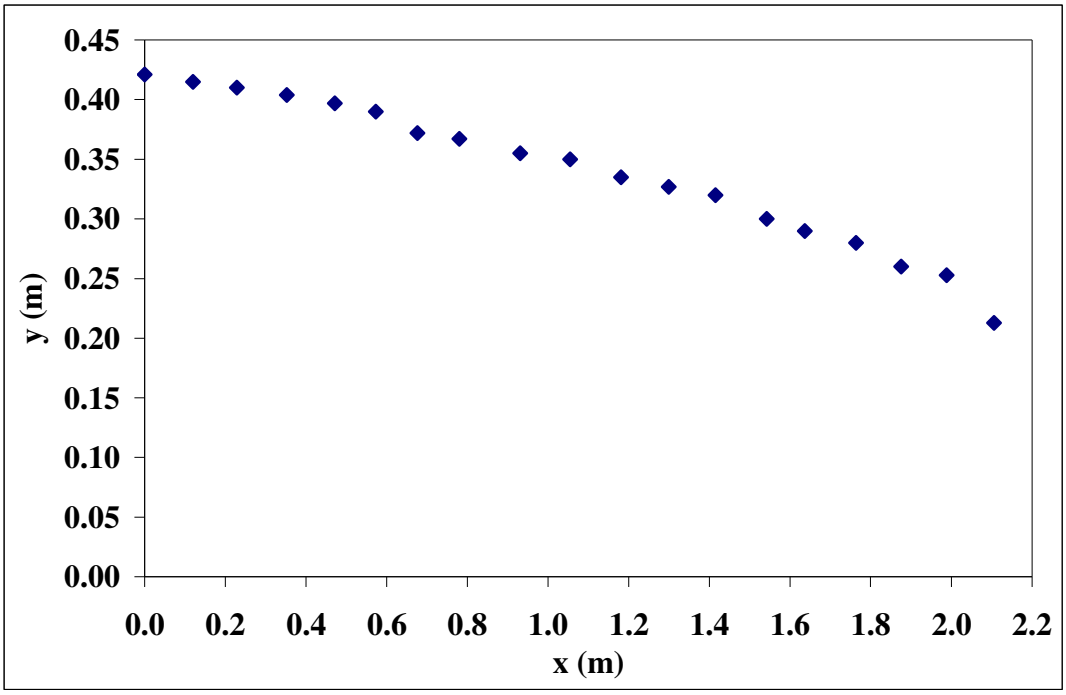

Figure 4.8 An example of non-Darcian flow profile

Table 4.5 Calculation of the weir porosity

$\forall_{total}$ (cm^3) =	561238.875
$\forall_{brick}$ (cm^3) =	517387.500
$\forall_{void}$ (cm^3) =	43851.375
$n = \frac{\forall_{void}}{\forall_{total}}$ =	**0.0781**

Table 4.6 Measurements for non-Darcian flow case

Measuring points	***x*(m)**	***y* (m)**
1	0.000	0.421
2	0.120	0.415
3	0.228	0.410
4	0.353	0.404
5	0.472	0.397
6	0.573	0.390
7	0.676	0.372
8	0.777	0.367
9	0.931	0.355
10	1.055	0.350
11	1.181	0.335
12	1.299	0.327
13	1.415	0.320
14	1.542	0.300
15	1.636	0.290
16	1.764	0.280
17	1.876	0.260
18	1.988	0.253
19	2.106	0.213

4.4 Concluding Remarks

Physical models are constructed for verification of mathematical models. In this thesis, numerical solution is used for mathematical modeling and it is tested by experimental investigation. In this chapter, experimental investigation in laboratory is explained. In the first part, information for experimental setup is given. In the following part, calculation and measurement of discharge is shown. In the last part, types of experiments and need for them is explained in detail.

CHAPTER 5

PRESENTATION, DISCUSSION AND COMPARISON OF THE RESULTS

The second objective of this thesis study is to verify the functionality of the numerical solution. In order to achieve this verification experimental studies are made. In the previous chapter, experiment conditions are explained. According to those conditions, several test scenarios are taken into consideration. In this chapter, all experimental data and numerical solutions for the same conditions are given. For the verification purpose, experimentally and numerically obtained water surface profiles are compared and presented in this section.

5.1 Introductory Remarks

Hydraulic conductivity of the porous medium used in experimental system is not known apriori. Hence, to compute this property, first type of experimental data and the calculation procedure given in hydraulic conductivity part are used. According to these, hydraulic conductivity is calculated as 0.23374 m/s.

Various geometric parameters and medium properties for both experimental study and numerical application are given in Table 5.1. Geometric permeability, k, can be calculated from hydraulic conductivity, K, by using the following equation:

$$k = \frac{K\nu}{g} \tag{5.1}$$

Moreover, c value indicated in Table 5.1 is obtained from the study conducted by Sidiropoulou et al. (2007). In that study, review of Forchheimer coefficients A_1 and A_2 obtained experimentally by various researches for different materials is presented in table. Value of coefficient c used in this thesis is calculated from A_1 and A_2 coefficients taken from that table.

In order to compare the results of numerical solution with those of experimental findings, the input values for numerical solution are set the same as the respective values for the experiments. By using the parameters presented in Table 5.1 and applying the flow chart given in Figure 3.3, flow through weir is obtained numerically. These results are compared with two different sets of experimental data.

Table 5.1 Parameter values and geometric properties of both channel and weir

Parameters	Value	SI Units
c =	0.29	
ν =	1.30E-06	m^2/s
T =	10	ºC
g =	9.81	m/s^2
n =	0.0781	
K =	0.23374	m/s
$k = K\nu/g$ =	3.10E-08	m^2
S_0 =	0.000	
$b_{channel}$=	0.675	m
b_{weir} =	0.675	m
$L_{channel}$ =	7.540	m
L_{weir} =	2.106	m
h_{weir} =	0.500	m
Δx =	0.100	m

5.2 Experimental, Numerical and Analytical Results for Darcian Flow

5.2.1 Comparison of Experimental Data with Analytical Solution for Darcy Flow

For verification of Darcy flow in the first type of experiments, the obtained data are compared with the analytical solution valid for Darcy law. The analytical solution used in this comparison is based on Dupuit assumption. These comparisons are shown in Figure 5.1, Figure 5.2, and Figure 5.3. As seen in these figures, experimental values are close to analytical ones. Experimental data are plotted against analytical ones to verify its closure to analytical solution. This verification can be seen in Figures 5.4, 5.5, 5.6, and 5.7.

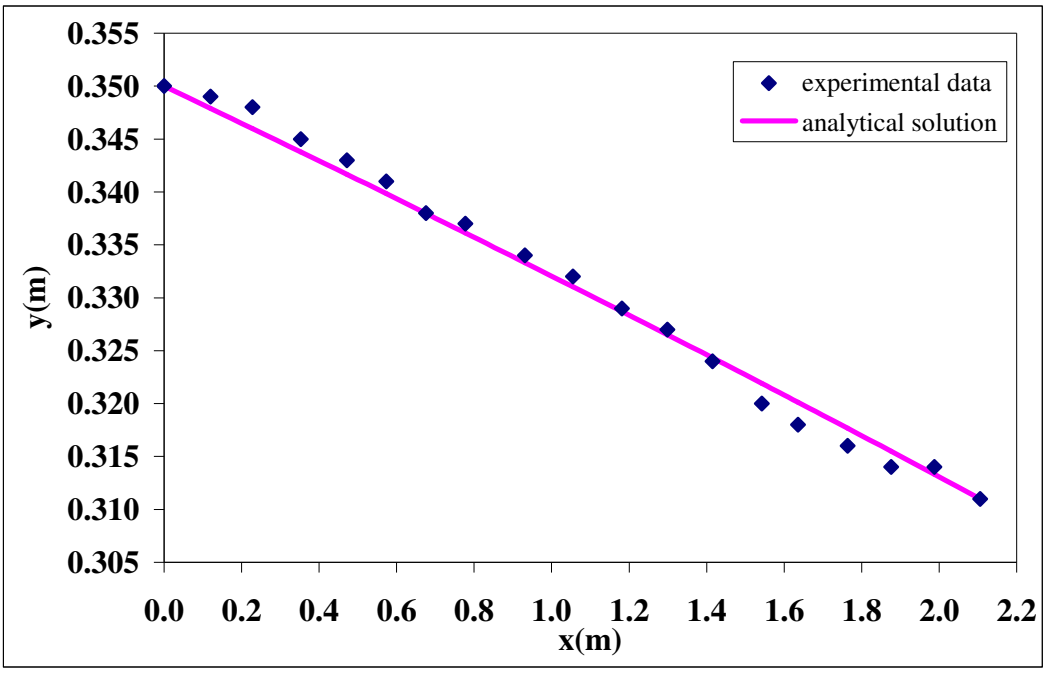

Figure 5.1 Graph of experimental data and analytical solution for Darcy flow (Experiment 1)

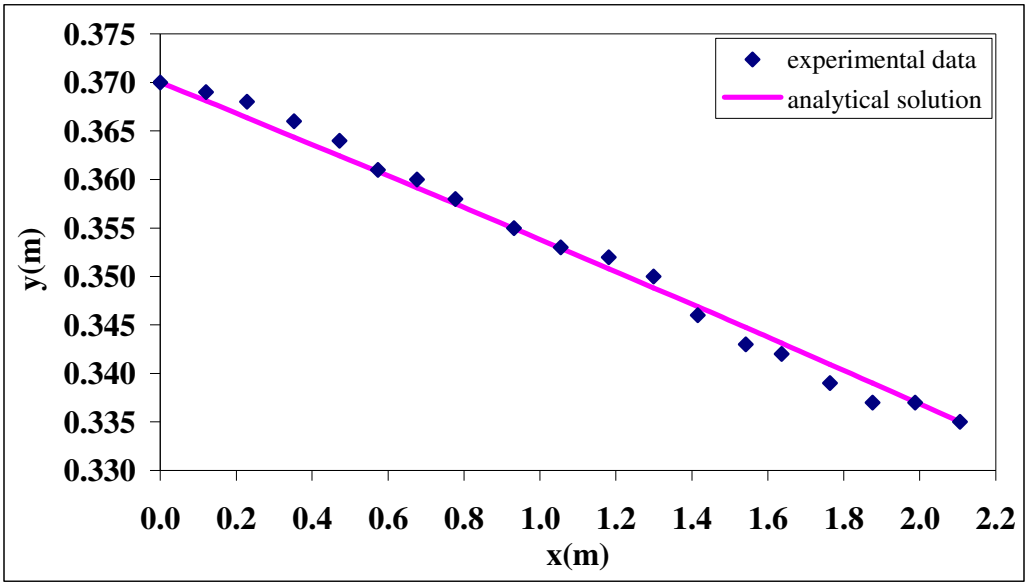

Figure 5.2 Graph of experimental data and analytical solution for Darcy flow (Experiment 2)

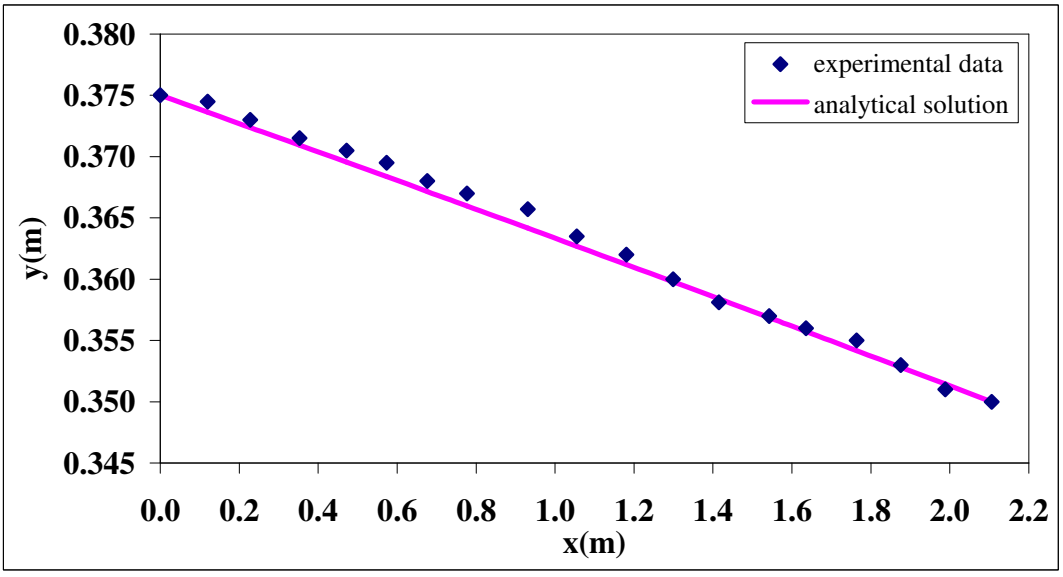

Figure 5.3 Graph of experimental data and analytical solution for Darcy flow (Experiment 3)

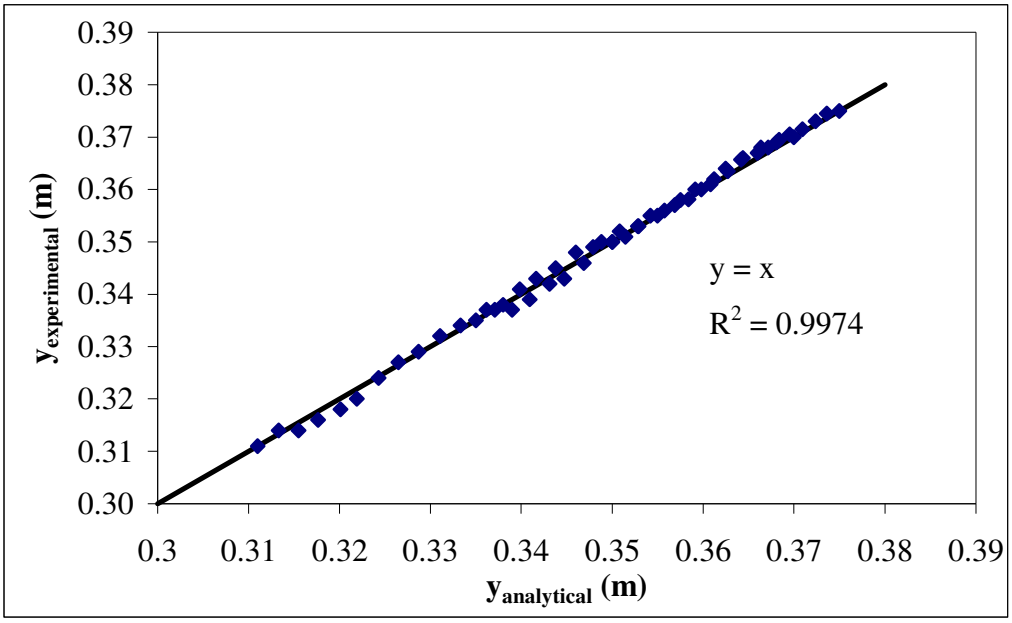

Figure 5.4 Graph of all experimental data versus analytical solutions

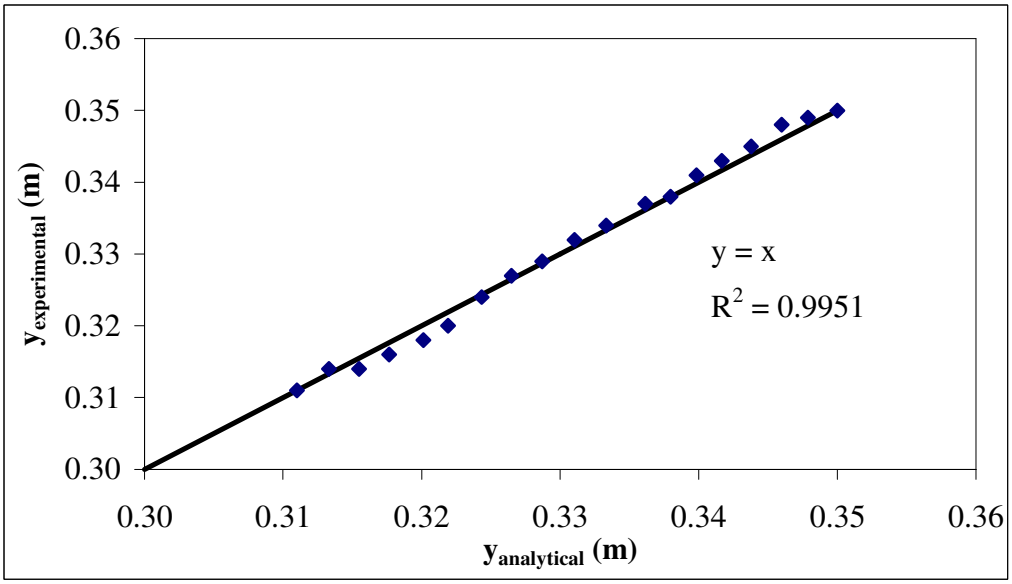

Figure 5.5 Graph of experimental data versus analytical solution for experiment 1

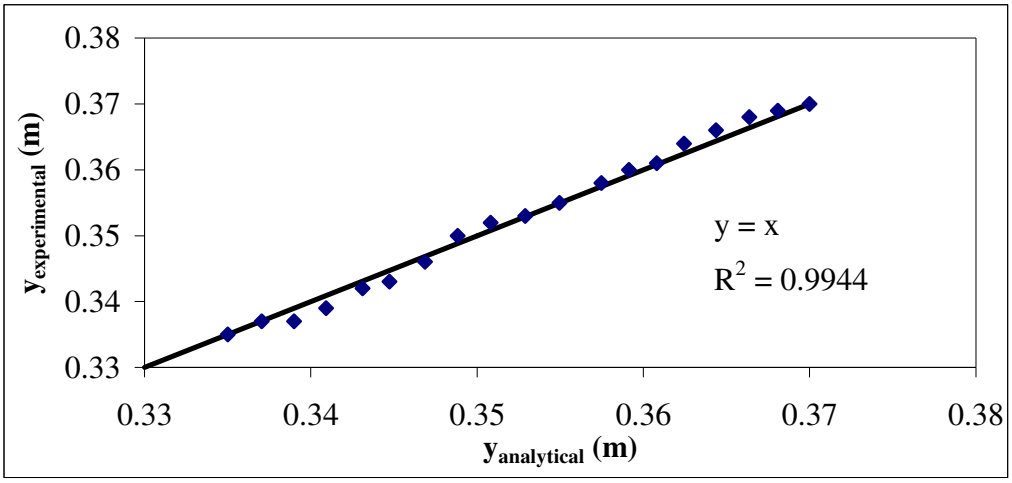

Figure 5.6 Graph of experimental data versus analytical solution for experiment 2

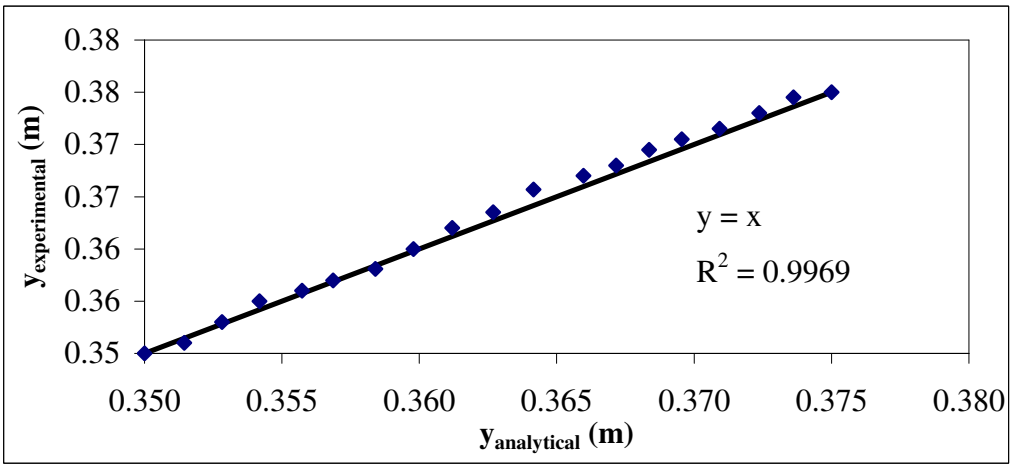

Figure 5.7 Graph of experimental data versus analytical solution for experiment 3

The results presented in Figures 5.1 through 5.7 shows that the use of the analytical solution of one-dimensional Darcian flow based on Dupuit assumption, for determination of the hydraulic conductivity, is justified. Consequently, the calculated hydraulic conductivity represents the conducting property of the porous medium used in this research work.

5.2.2 Comparison of Numerical Solution with Experimental Data

As mentioned before, in the absence of the term $\{c/g\sqrt{k}\}$, Equation (2.17) becomes equivalent to Darcy's law. Therefore, c value is set to zero to obtain water surface profiles with the numerical method for Darcy flow. For this Darcian flow, in Figure 5.8, Figure 5.9, and Figure 5.10, a comparison of the experimentally and numerically obtained water surface profiles are shown.

The results in Figures 5.8, 5.9, and 5.10 indicate that the numerical solution developed for non-Darcian flow, may also be used for Darcian flow as a special case. This inference could have been enhanced with the help of the root mean square error analysis between experimental and numerical results. However, measuring points of experimental data and computational points of numerical solution do not exactly coincide. Therefore, an indirect verification is used for the numerical solution. In the previous section, verification of analytical solution is done as shown in Figure 5.4. By using analytical solution, numerical solution is verified with the help of root mean square error analysis. This verification is shown in Figure 5.11. The results of 1-D analytical solution very well comply with both numerical and experimental results.

The water head elevations determined experimentally in some parts do not exactly coincide with numerically obtained ones. The reason may be that the assumption of homogeneity of porous medium throughout the whole length of weir is not fully satisfied. Bricks are not perfectly identical in size and shape. Consequently, this difference may affect the homogeneity. As a result, the deviation in figures may be due to heterogeneity of the system.

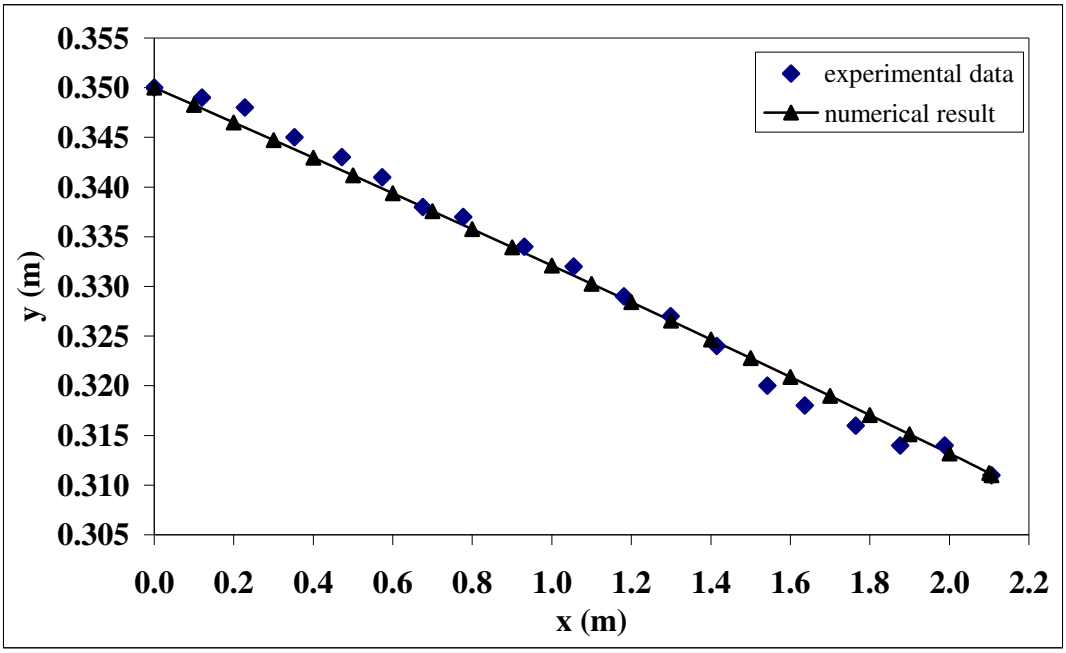

Figure 5.8 Graph of numerical solution and experimental data for Darcy flow (Experiment 1)

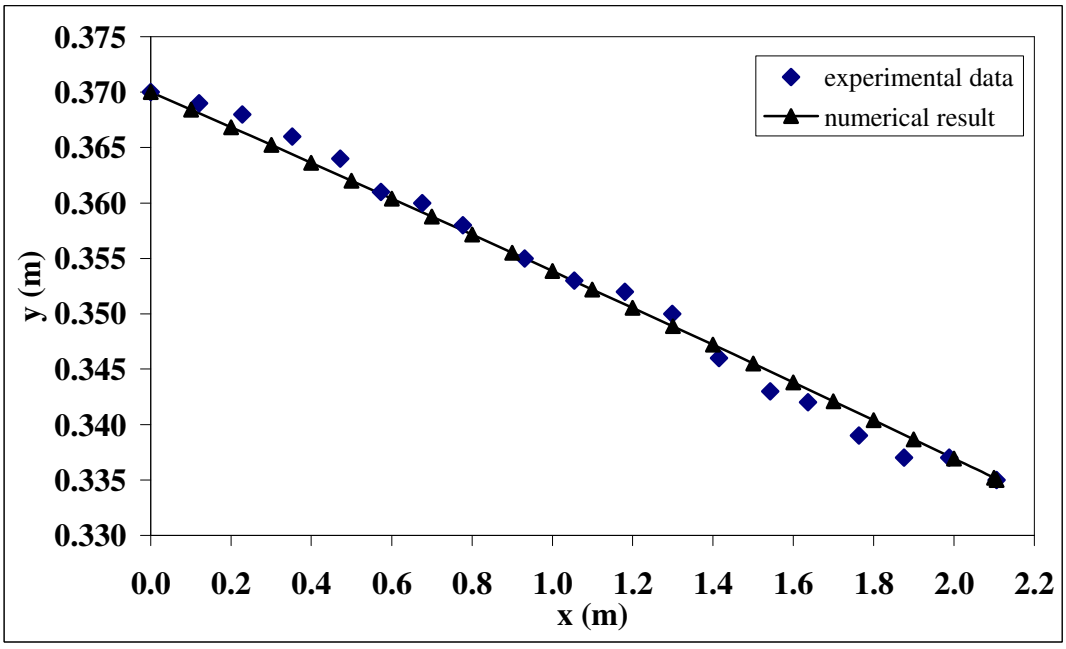

Figure 5.9 Graph of numerical solution and experimental data for Darcy flow (Experiment 2)

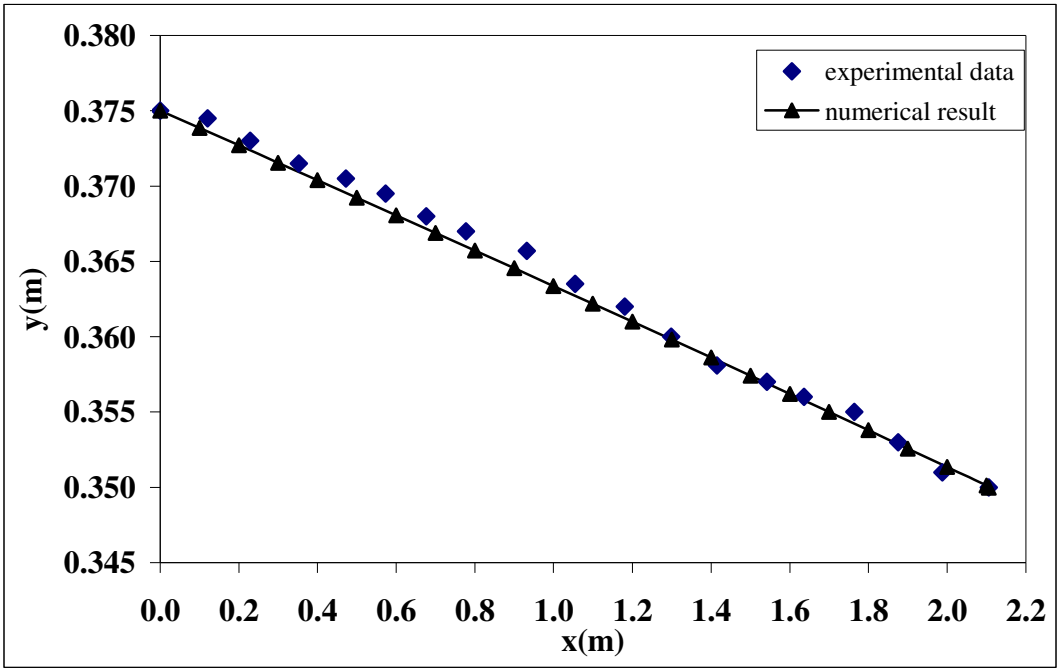

Figure 5.10 Graph of numerical solution and experimental data for Darcy flow (Experiment 3)

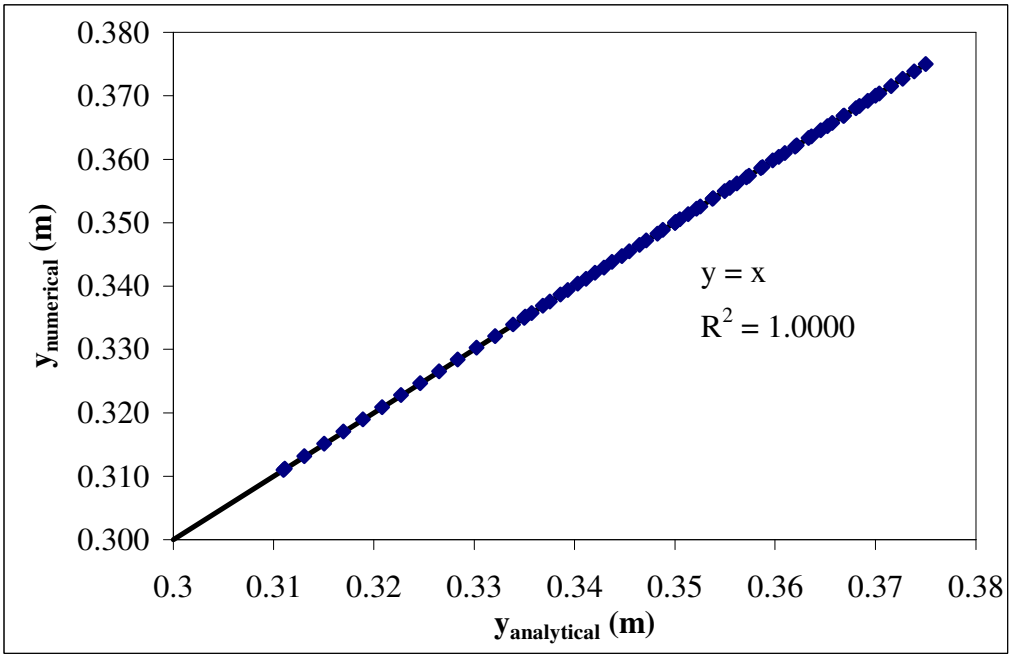

Figure 5.11 Graph of numerical solutions versus analytical solutions

5.3 Experimental and Numerical Results for Non-Darcian Flow

5.3.1 Comparison of Experimental and Numerical Results based on Forchheimer Equation

The second group of experiments with non-Darcian flow conditions is carried out to test and verify the proposed numerical method. The numerically obtained water surface elevations are shown in Figure 5.12 and Figure 5.13, and related data are given in Table 5.2. The comparisons of these two water surface profiles with corresponding experimental results are presented in Figure 5.14 and Figure 5.15. Furthermore, all the remaining calculated and measured water surface profiles are presented in Appendix A. A reasonable and satisfactory agreement is observed from these plots. This is considered to be a sufficient confidence in using the proposed numerical model.

Table 5.2 Water head elevations determined by numerical solution

x(m)	y_{exp4} (m)	y_{exp5} (m)
0.000	0.421	0.480
0.100	0.414	0.475
0.200	0.407	0.470
0.300	0.400	0.464
0.400	0.393	0.459
0.500	0.385	0.453
0.600	0.377	0.448
0.700	0.370	0.442
0.800	0.361	0.437
0.900	0.353	0.431
1.000	0.344	0.425
1.100	0.335	0.419
1.200	0.326	0.413
1.300	0.316	0.406
1.400	0.306	0.400
1.500	0.295	0.393
1.600	0.284	0.387
1.700	0.272	0.380
1.800	0.260	0.373
1.900	0.246	0.366
2.000	0.231	0.358
2.100	0.215	0.351
2.106	0.213	0.350

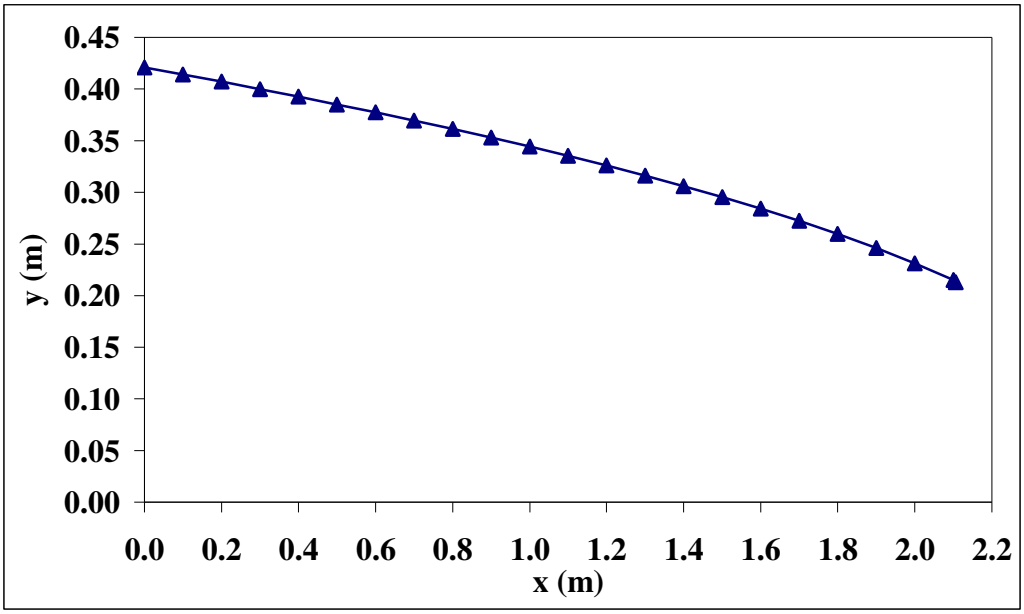

Figure 5.12 Graph of numerical solution for non-Darcian flow (Experiment 4)

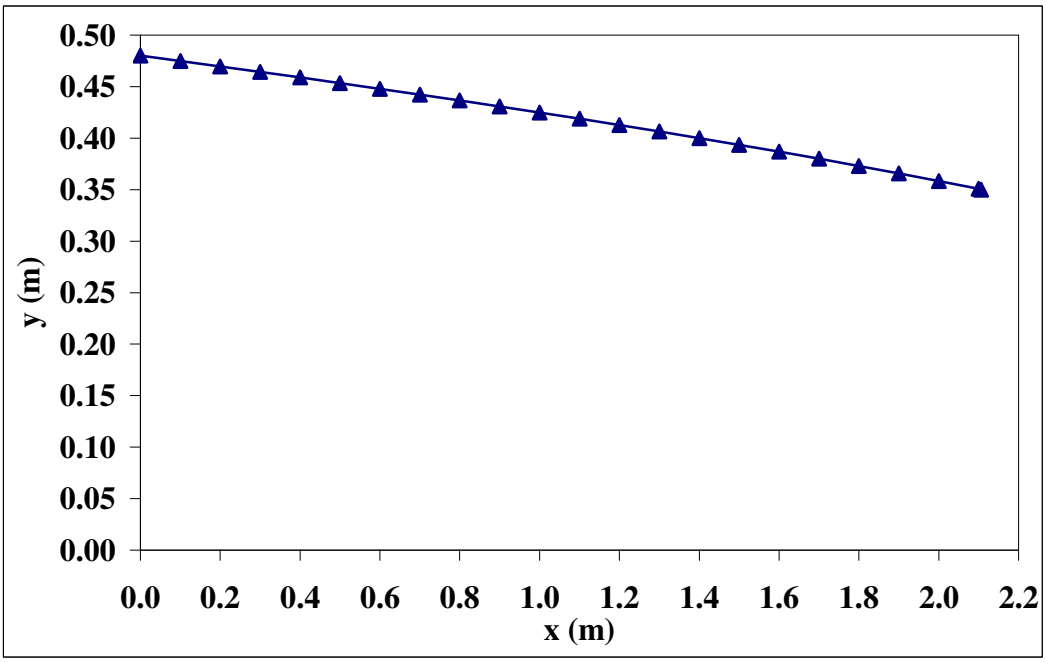

Figure 5.13 Graph of numerical solution for non-Darcian flow (Experiment 5)

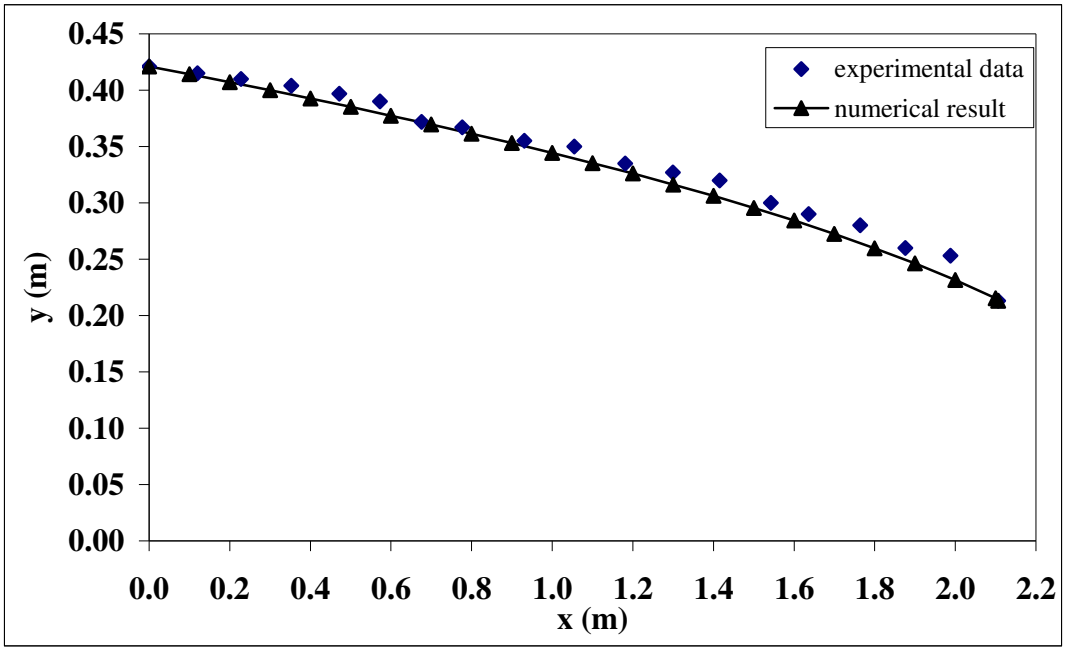

Figure 5.14 Graph of numerical solution and experimental data for non-Darcian flow (Experiment 4)

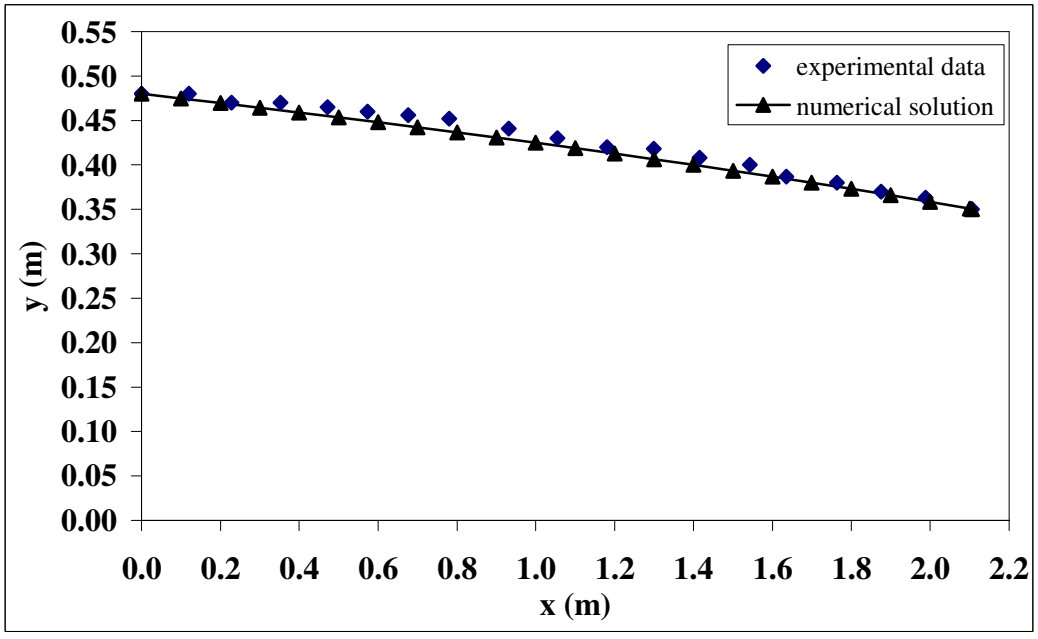

Figure 5.15 Graph of numerical solution and experimental data for non-Darcian flow (Experiment 5)

5.3.2 Comparison of Different Non-Darcian Flow Equations

For calculation of water surface profile of the flow through porous media, open channel algorithm is used. In this algorithm, as mentioned before, the longitudinal variation in water depth is no longer governed by the roughness of the streambed, as in the case for open channel flow, but by the characteristics of the coarse porous media. Consequently, as discussed in Chapter 2, earlier studies used Stephenson and Wilkins' equations [Equation (2.8) and Equation (2.11)] for the evaluation of the friction slope, S_f, in the differential equation of gradually varied flow. However, in this thesis work Forchheimer relation in which laminar and turbulent components of flow resistance in the porous body are taken into consideration is preferred. Obtained water surface profiles for these three equations and experimental data are presented in Figure 5.16. From this figure, it can be concluded that among all these three numerical water surface profiles the one obtained by using Forchheimer relation presents approximate values to the ones obtained experimentally.

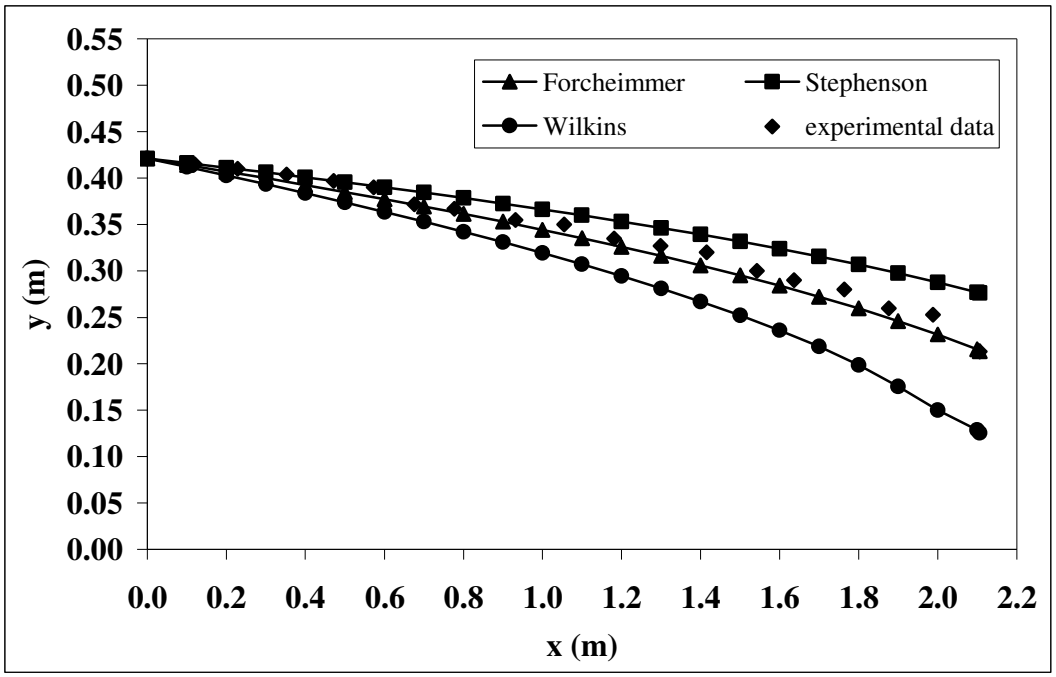

Figure 5.16 Water surface profiles obtained using different numerical solutions

5.4 Discussion

This study presents a numerical solution for one-dimensional and non-Darcian flow through rockfill. The governing equations have been derived from the energy equation. The fluid velocity through porous medium is often too high for linear Darcian flow to be valid. The higher the velocity, the higher the non-linearity. Therefore, the governing equation is modified using Forchheimer relation, which includes both laminar and turbulent components of flow.

The governing equation is solved numerically. The main aspect in the numerical solution of such a weir problem is the modeling of water surface profile. The modeling is done by using trapezoidal method of integration. The verification of numerical model is achieved in two stages. In the first stage, the accuracy of the numerical solution has been verified by comparing it to available analytical solution for the special case of Darcian flow through rockfill. The numerical solution has given good approximation to analytical one.

In the second stage, the numerical solution has been verified by conducting experimental investigation. Upon comparison of the results, water surface profiles are calculated numerically with setting the input values the same as the respective ones for experiments. The plots of both numerical and experimental profiles are presented. According to the graphs plotted, numerical solution and experimental data give closer results. From all the graphs, it can be concluded that numerical solution gives lower values than experimental data. It can be due to experimental measurement error of water head elevation readings and discharge. In addition, the reason may be the error of numerical solution procedure. Iteration method and trapezoidal rule can cause some errors. Except from these reasons, parameters used in numerical solution may lead to these lower values. Actually, hydraulic conductivity is affected by temperature change. Thus, correction of conductivity for temperature effect may solve the error.

It is also observed from the results that, the controlling parameters are water depths at upstream and downstream sides of the weir, discharge through porous media, the weir and channel length, and hydraulic conductivity of the system.

Furthermore, from calculated Froude number values for all experiments it can be concluded that all conducted flows are subcritical flow. Related data for the calculation of Froude numbers are given in Table 5.3.

Table 5.3 Froude numbers for all experiments

Flow type	Exp no	y_u (m)	y_d (m)	Q (m^3/s)	Fr_u	Fr_d	Fr_u (porous)	Fr_d (porous)	y_c (m)
Darcy	1	0.350	0.311	0.00101	0.0023	0.0028	0.0006	0.0006	0.0061
	2	0.370	0.335	0.00097	0.0020	0.0024	0.0006	0.0006	0.0059
	3	0.375	0.350	0.00092	0.0019	0.0021	0.0006	0.0005	0.0057
Non-Darcy	4	0.421	0.213	0.00438	0.0076	0.0211	0.0028	0.0020	0.0163
	5	0.480	0.350	0.00384	0.0055	0.0088	0.0026	0.0022	0.0149
	6	0.403	0.083	0.00438	0.0081	0.0866	0.0027	0.0012	0.0163
	7	0.400	0.083	0.00425	0.0079	0.0841	0.0027	0.0012	0.0159
	8	0.316	0.190	0.00195	0.0052	0.0111	0.0011	0.0008	0.0095
	9	0.320	0.210	0.00174	0.0045	0.0086	0.0010	0.0008	0.0088
	10	0.443	0.335	0.00308	0.0049	0.0075	0.0020	0.0018	0.0129
	11	0.425	0.330	0.00308	0.0053	0.0077	0.0020	0.0017	0.0129
	12	0.430	0.338	0.00308	0.0052	0.0074	0.0020	0.0018	0.0129
	13	0.386	0.310	0.00216	0.0043	0.0059	0.0013	0.0012	0.0101

5.5 Concluding Remarks

In order to achieve second objective of this thesis, verification of numerical solution with the help of experimental investigation is done in this chapter. For two sets of experiments mentioned in previous chapter, all numerical solutions for each one are given. Comparisons of water surface profiles that are obtained numerically and experimentally are shown in figures in this chapter.

CHAPTER 6

CONCLUSION AND RECOMMENDATION

6.1 Summary

In recent decades, an emphasis is given on the sustainable use of water resources and ecologically friendly solution in various disciplines. The rubble mound weir allows the streamwise migration of aquatic life, because the body is porous. As compared to the conventional impermeable weirs constructed of materials such as concrete, the permeable rubble mound weir might serve a structure with minimal negative impact on the river environment and it is more environmentally friendly. However, available information of flow through permeable weirs is insufficient; thus, water surface profiles through these structures should be modeled for design of that kind of structures. Therefore, detailed literature survey is investigated. According to this literature investigation, necessity for this thesis is pointed out.

For the solution of the problem, related background information is summarized. In literature, Darcy and non-Darcian flow equations were previously studied by various researches. Most common relations were obtained by Forchheimer and Izbash. Ward (1964), Stephenson (1979), and Wilkins (Bari and Hansen, 2002) had successfully proposed equations to those relations. In this thesis, unlike previous studies, Forchheimer relation is used for modeling of flow through porous media. Governing equation regarding this type of flow is obtained.

Moreover, the resulting equation is solved numerically. Need for numerical solution for water surface profile computation is explained in detail. Available methods of integration for gradually varied flow in literature are briefly reviewed. Trapezoidal method of integration is chosen and related information of this method is given. Main equation of this thesis approach is also identified. After that, the procedure used in modeling the non-Darcian flow profile is explained step by step.

The second objective of this thesis study is to verify the numerical solution. In order to achieve this verification physical model is constructed in laboratory. The experimental investigation of the weir model is done. First, experimental setup is explained in detail. Then, measurements of water head elevations and discharges are shown for each experiment. In that part of this thesis, experiment conditions are pointed out. Two groups of test scenarios are taken into consideration. Moreover, experimentally and numerically obtained water surface profiles are presented and compared.

6.2 Conclusion

From this study the following conclusions are reached:

1. The results of the analytical solution and the experimental data for Darcian flow indicate that the experimentally determined hydraulic conductivity reflects almost accurately the hydraulic characteristics of the porous media.

2. Small deviations of experimental results may be caused by local heterogeneity due to non-milimetric placement of bricks and non-milimetric fabrication of brick sizes.

3. A special case of numerical solution, that is Darcian flow case, is verified with physical model in laboratory.

4. Common point in numerical and analytical solutions is that they are based on Dupuit assumption.

5. The experimental results are in a very good agreement with numerical results for non-Darcian one-dimensional steady flow through porous medium.

6. As an overall conclusion, it may be stated that the outcome of this research work has been a contribution to the understanding of the flow behavior through rockfills. This work may be used in design problems. The flow through weir depends on initial water depth, y_1, final water depth, y_2, length of weir, L, and discharge passing through the system, Q. For example, if initial and final water depths are known, satisfactory values of length of weir and discharge can be calculated by trial and error method.

6.3 Recommendation for Future Work

Because of the limitations in scope and for time, some complementary works of this research could not have been studied. In this study, only one-dimensional flow is considered. The study can be extended to two-dimensional flow.

After comparison of results in this thesis, it is believed that further experimental investigation will be needed to strengthen the verification of the proposed numerical method used in this work. This further experimental work can be usage of different material for porous media such as different size of bricks, blocks of concrete, very coarse gravel and cobbles, etc. Furthermore, an alternative approach can be the governing differential equation obtained by combining the continuity equation and Forchheimer relation. In that approach, numerical solution of the resulting equation may be based on finite difference or finite element approximation.

In this thesis, only flow through weir is studied and modeled. However, for higher values of flowrate overflow conditions will occur. All possible flow conditions should be examined in future works. In the light of the obtained and observed water surface profiles, potential of the permeable weir as an energy dissipating system should be investigated.

REFERENCES

Addison, H., "A Treatise on Applied Hydraulics", New York, John Wiley & Sons Inc., 1954.

Ahmed, N., and Sunada, D., "Nonlinear flow in porous media", J. Hydr. Div., ASCE, 1969, 95(6), pp. 1847–1857.

Arbhabhirama, A., and Dinoy, A., "Friction Factor and Reynolds Number in Porous Media Flow", Journal of Hydraulic Division, ASCE, Vol. 99, No.HY6, June 1973, pp. 901-911.

Banna, M. S., "Experimental and Numerical Analysis of Unsteady One-Dimensional Groundwater Flow in a Non-Uniform Aquifer", M.S. Thesis, Civil Engineering Department, Middle East Technical University, Ankara, Turkey, July 1997.

Bari, R.; Hansen, D., "Application of Gradually-Varied Flow Algorithms To Simulate Buried Streams", Journal of Hydraulic Research, 2002, 40:6.

Basak, P., "Steady non-Darcian Seepage through Embankments", Journal of Irrigation and Drainage, ASCE, December 1976, pp. 435-443.

Bear, J., "Hydraulics of groundwater", McGraw-Hill, 1979.

Blake, F., "The resistance of packing to fluid flow", Trans. Am. Soc. Chemical Engrg., 1923, 14, 415.

Bordier, C. and Zimmer, D., "Drainage Equations and Non-Darcian Modeling in Coarse Porous Media or Geosynthetic Materials", Journal of Hydrology, 2000, Vol. 228, pp. 174-187.

Burke, S., and Plummer.W., “Gas flow through packed columns”, Ind. Engr. Chem., 1928, 20, 1196.

Carman, P., “Fluid flow through granular beds”, Trans. Inst. of Chemical Engrg., 1937, 15, 150.

Chow, V. T., “Open Channel Hydraulics”, McGraw–Hill, New York, 1959.

Darcy, H., “Les fontaines publiques de la vile de Dijon”, Victor Dalmont, Paris, 1856 (in French).

Dudgeon, C.R., “An Experimental Study of Flow through Coarse Granular Materials”, La Houille Blanche, 1966, Vol.21.

Engelund, R., “On the Laminar and Turbulent Flow of Ground Water through Homogeneous Sand” Transactions, Danish Academy of Technical Science, 1953, No.3.

Ergun, S., and Orning, A., “Fluid flow through randomly packed columns and fluidized beds”, Ind. and Engrg. Chem., 1949, 41(6), pp. 1179–1184.

Ergun, S., “Fluid flow through packed columns”, Chem. Engr. Prog., 1952, 43(2), pp. 89–94.

Fair, G., and Hatch, L., “Fundamental factors governing the streamline flow of water through sand”, J. AWWA, 1933, 25, 1551.

Forchheimer, P., “Wasserbewegung durch Boden”, Forschtlft ver. D. Ing., 1901, 45, pp. 1782–1788 (in German).

French, R. H., “Open Channel Hydraulics”, McGraw–Hill, New York, 1986.

Hannoura, A. A. and McCorquodale, J., “Rubble Mounds: Hydraulic Conductivity Equation”, Journal of Waterway, Port, Coastal and Ocean Engineering, ASCE, 1985, Vol.111, No.5, pp. 783-799.

Hansen, D., Garga, V. K., and Townsend, D. R., "Selection and application of a one-dimensional non-Darcy flow equation for two dimensional flow through rockfill embankments", Can. Geotech. J., 1994, 32(2), pp. 223–232.

Henderson, F. M. "Open Channel Flow", New York, Macmillan Publishing Co Inc, 1966.

Hubbert, M., "Darcy's law and the field equations of the flow of underground fluids", AIME Petr. Trans., 1956, 207, pp. 222–239.

Irmay, S., "On the theoretical derivation of Darcy and Forchheimer formulas", Trans. Am. Geophys. Union, 1958, 39(4), pp. 702–707.

King, H.W., "Handbook of Hydraulics", New York, McGraw Hill Book Company, Inc, 1954.

Korkmaz, S., "Seepage From Detention Basins to Groundwater Table", M.S. Thesis, Civil Engineering Department, Middle East Technical University, Ankara, Turkey, September 2002.

Kovacs, G., "Relationship between Velocity Of Seepage and Hydraulic Gradient in the High Velocity Zone", Proceedings of the XIII Congress, IAHR, Vol.4, Kyoto, Japan, September 1969.

Kozeny, J., "Ueger kapillare Leitung des Wassers im Boden [On capillary conduction of water in soil]", Sitzungsbericht, Akad. Wiss., Vienna, Vienna, Austria, abt. IIIa, 1927a, 136, 276.

Kozeny, J., "Ueger kapillare Leitung des Wassers im Boden [On capillary conduction of water in soil]", Wasserkraft Wasserwirtschaft, 1927b, 22, 67 (in German).

Kureksiz, O. and Onder, H., "Use of Forchheimer Equation in the Analysis of Water Surface Profile through Rubble Mound Weir", III.Ulusal Su Mühendisliği Sempozyumu, September 2007, pp. 87-97.

Kureksiz, O. and Onder, H., “Numerical and Physical Modeling of Flow through Rubble Mound Weir as a Water Use Facility”, International Conference on Fluvial Hydraulics, River Flow 2008 Izmir, Turkey, September 2008.

Li, B., Garga V.C., and Davies M.H., “Relationships for non-Darcy flow in rockfill”, Journal of Hydraulic Engineering, February 1998, Vol.124, No.2, pp. 206-212.

Maeno S., Michioku, K., Morinaga, S., and Ohnishi, T., “Hydraulic characteristics of a rubble mound weir and its failure process”, 5th ICHE Conference, Theme D, 2002.

Martins, R., “Turbulent seepage flow through rockfill structures”, Water Power and Dam Construction, March 1990, 90, pp.41-45.

McCorquodale, J.A., Hannom, A.,and Nasser, M. S., “Hydraulic conductivity of rockfill”, Journal of Hydraulic Research, 1978, 16(2), pp. 123-137.

Michioki, K., Maeno, S.,and Haneda, M., “Discharge Through A Permeable Rubble Mound Weir”, Journal of Hydraulic Engineering © ASCE, 2005, 131:1(1).

Nutting, P., “Physical analysis of oil sands”, Bull. Am. Assn. Petr. Geol., 1930, 14, 1337.

Pickard, W. F., “Solving the Equations of Uniform Flow”, Journal of Hydraulics Division, ASCE, 1963, Vol.89, No.4, pp. 23-37.

Polatel, C., “Unsteady One-Dimensional Groundwater Flow in a Non-Uniform Aquifer With Various Field Boundary Conditions”, M.S. Thesis, Civil Engineering Department, Middle East Technical University, Ankara, Turkey, January 2000.

Prasad, R., “Numerical Method of Computing Flow Profiles”, Journal of the Hydraulic Division © ASCE, 1970, 96(HYI), pp. 75-86.

Qian, J.; Zhan, H.; Luo, S.; Zhao, W., “Experimental Evidence of Scale-Dependent Hydraulic Conductivity For Fully Developed Turbulent Flow in a Single Fracture”, Journal of Hydrology, 2007, 339, pp. 206-215.

Scheidegger, A., “The physics of flow through porous media”, Macmillan, New York, 1960.

Sidiropoulou, M.G., Moutsopoulos, K.N., and Tsihrintzis, V.A., “Determination of Forchheimer Equation Coefficients a and b”, Hydrological Processes, 2007, 21, pp. 534-554.

Stephenson, D., “Rockfill in Hydraulic Engineering”, Elsevier Scientific, Amsterdam, The Netherlands, 1979.

Sunada, D., “Turbulent flow through porous media”, Contribution No. 103, Water Resour. Center, University of California, Berkeley, 1965.

Taylor, D.W., “Fundamentals of soil mechanics”, John Wiley & Sons, Inc., New York, N.Y, 1948.

Todd, D. and Mays, L. W., “Groundwater Hydrology”, John Willey & Sons, Inc., NJ, 2005.

Trussell, R.R., and Chang, M., “Review of flow through porous media as applied to head loss in water filters”, Journal of Environmental Engineering, 1999, Vol. 125, No. 11, pp. 998-1006.

Vafai, K., “Handbook of porous media”, Marcel Dekker, New York, 2000.

Venkatamaran, P. and Rao, P. R. M., “Darcian, Transitional and Turbulent Flow through Porous Media”, Journal of Hydraulic Engineering, August 1998, pp. 840-846.

Ward, J. C., “Turbulent flows in porous media”, Journal of Hydraulic Division © ASCE, 1964, 90(5), pp. 1–12.

Wyckoff, R., Botset, G., Muskat, M., and Reed, D., “The measurement of permeability of porous media for homogeneous fluids”, Rev. Scientific Instruments, 1933, 4, 394.

Yılmaz, B., “Development and Validation of Two-Dimensional Depth-Averaged Free Surface Flow Solver”, M.S. Thesis, Civil Engineering Department, Middle East Technical University, Ankara, Turkey, September 2003.

Zimmerman, R.W., Al-Yaarubi, A., Pain, C.C., and Grattoni, C.A., “Non-linear regimes of fluid flow in rock fractures”, Int. J.Rock Mech. Min. Sci., Vol.41, No.3, paper1A27, CD-ROM, ©2004 Elsevier Ltd.

APPENDIX A

EXPERIMENTAL AND NUMERICAL DATA

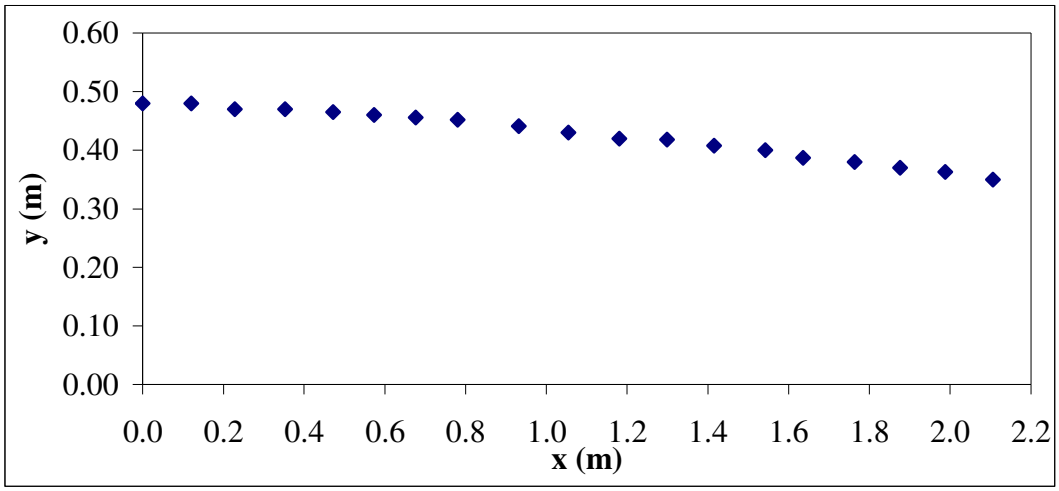

Figure A.1 Water surface profile measured experimentally for experiment 5

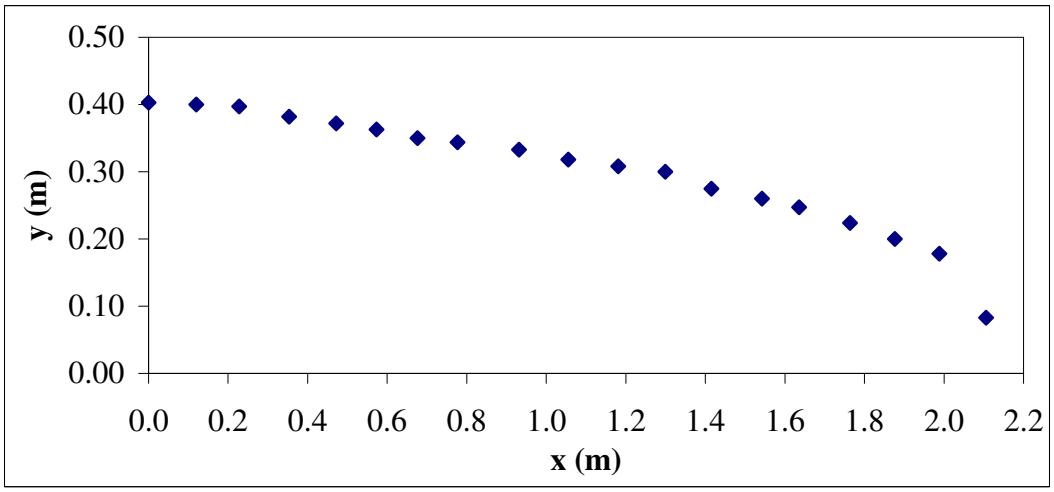

Figure A.2 Water surface profile measured experimentally for experiment 6

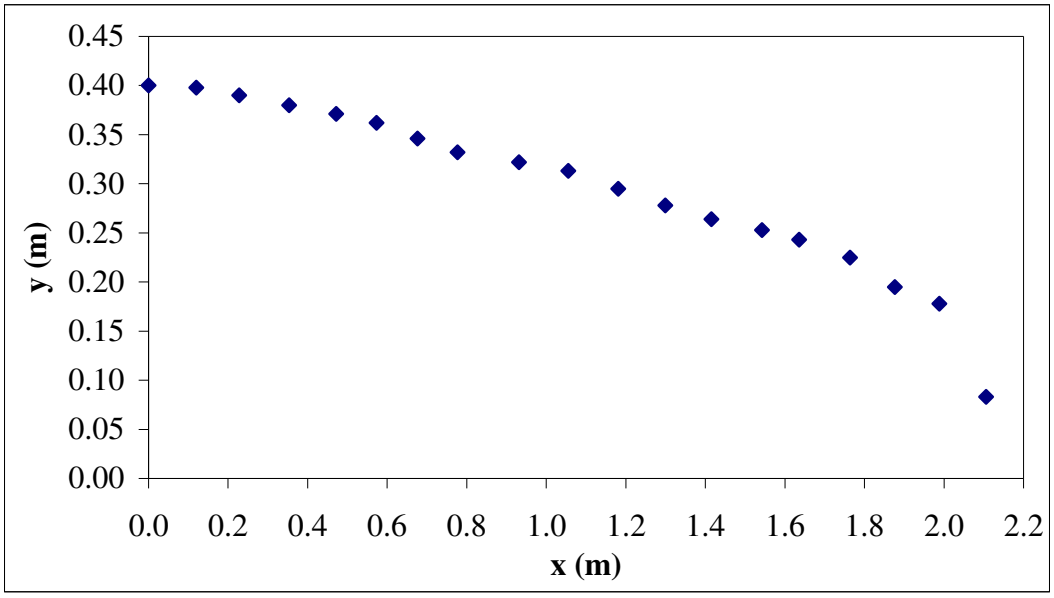

Figure A.3 Water surface profile measured experimentally for experiment 7

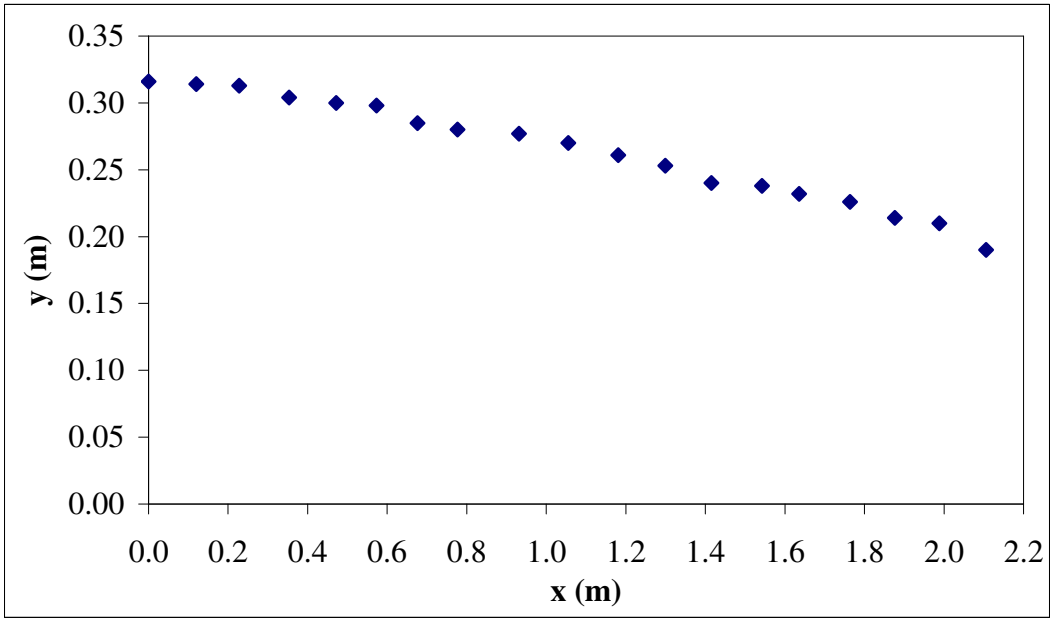

Figure A.4 Water surface profile measured experimentally for experiment 8

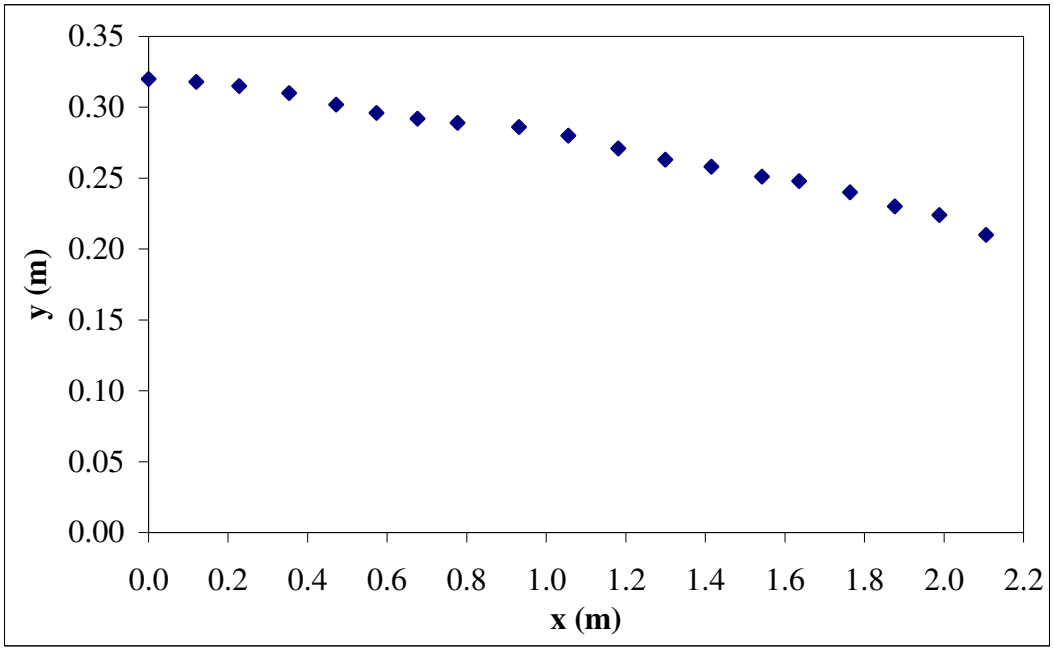

Figure A.5 Water surface profile measured experimentally for experiment 9

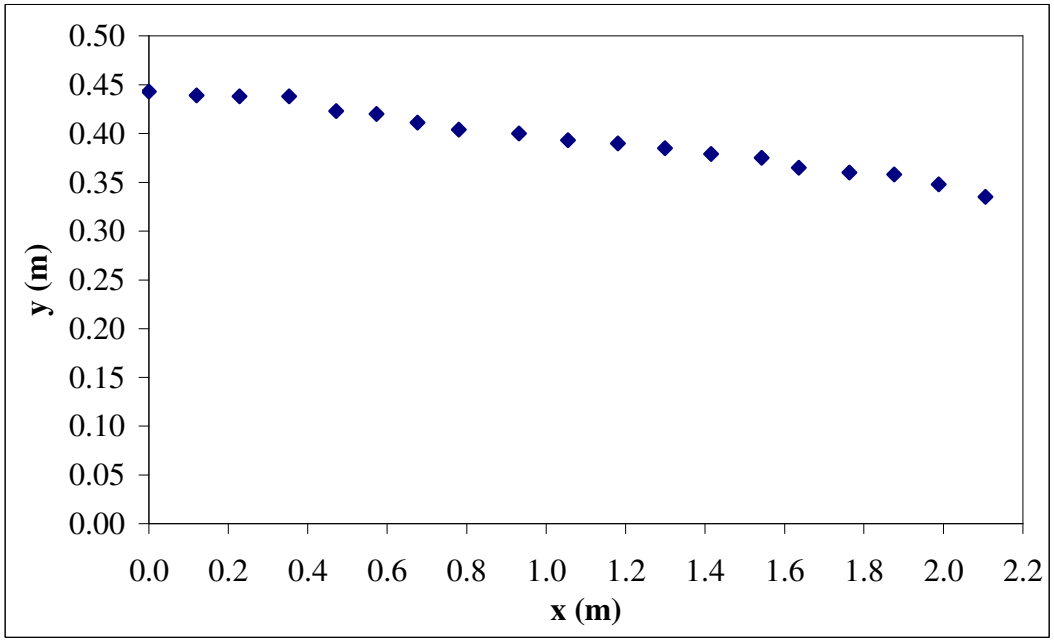

Figure A.6 Water surface profile measured experimentally for experiment 10

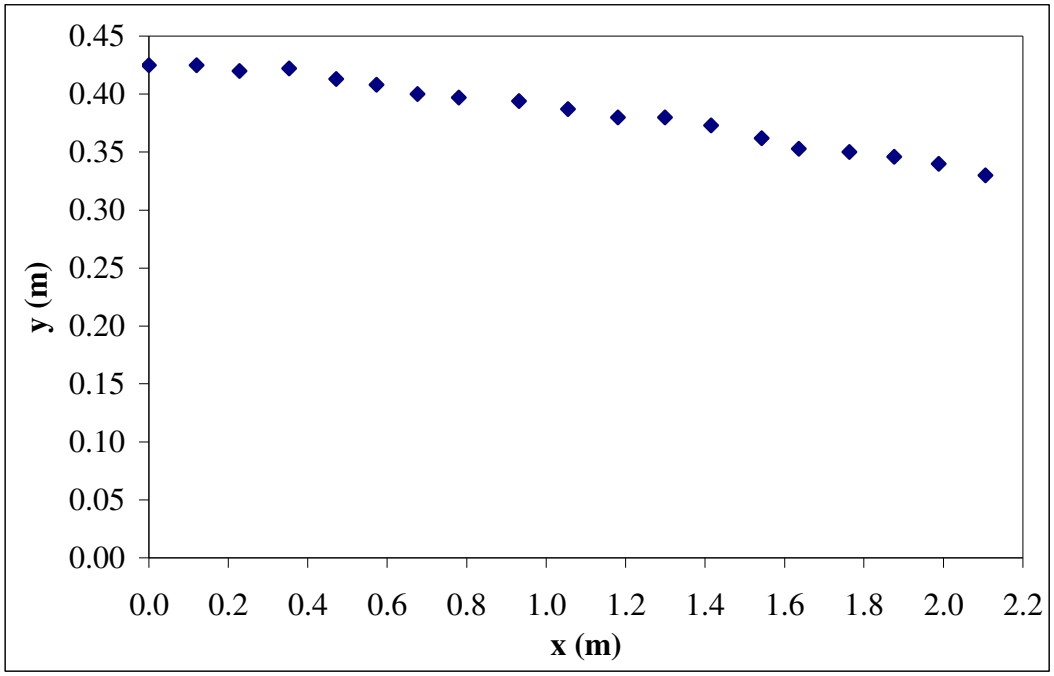

Figure A.7 Water surface profile measured experimentally for experiment 11

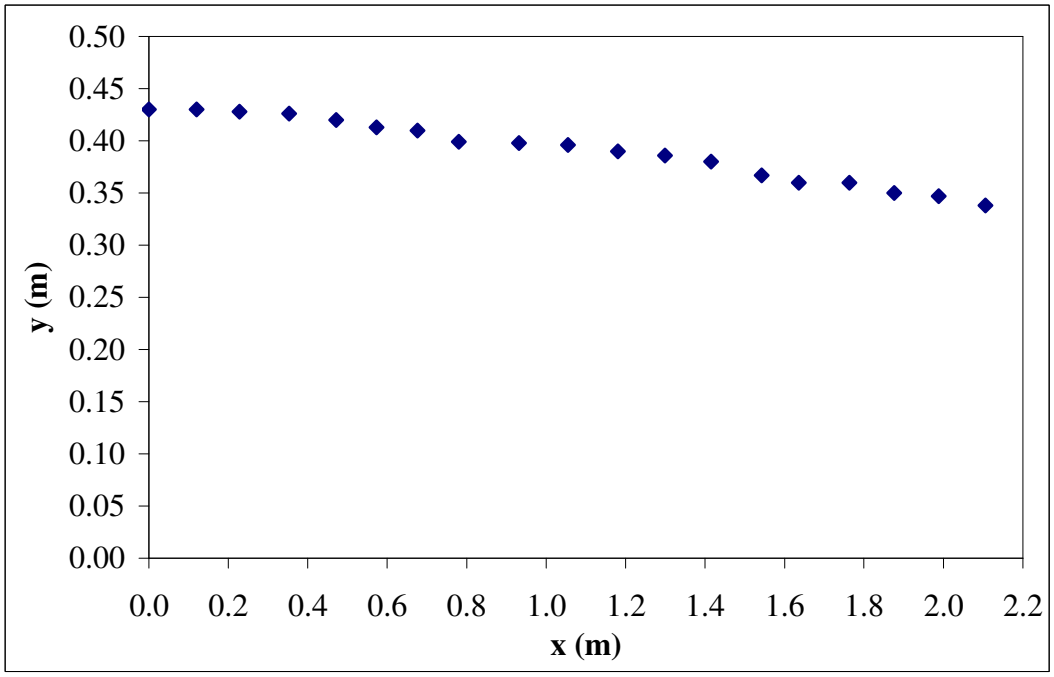

Figure A.8 Water surface profile measured experimentally for experiment 12

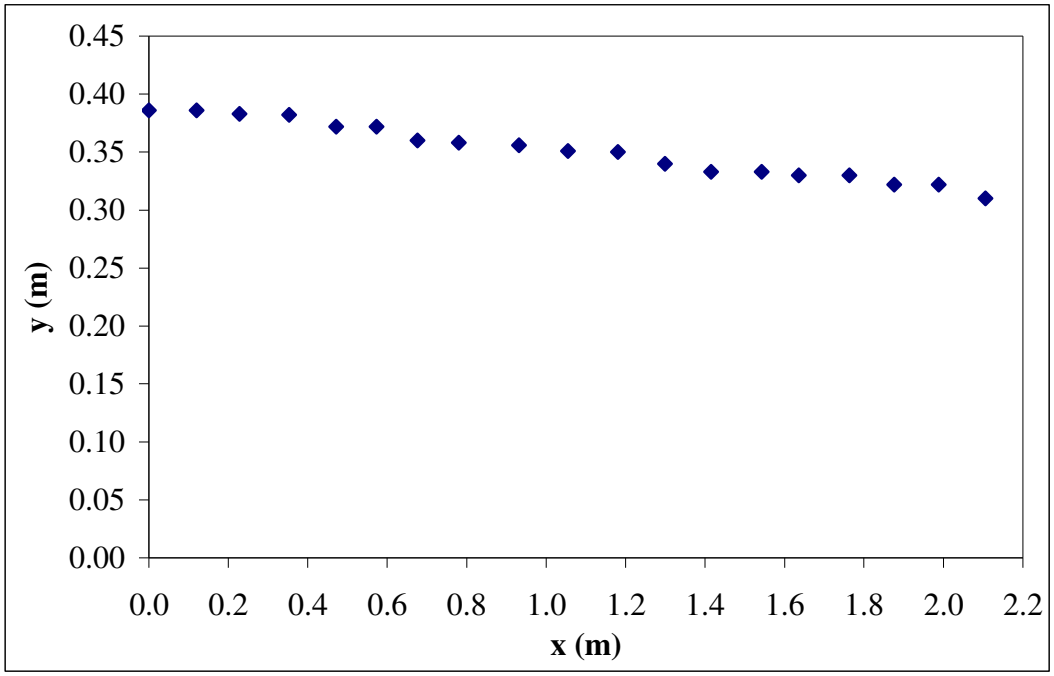

Figure A.9 Water surface profile measured experimentally for experiment 13

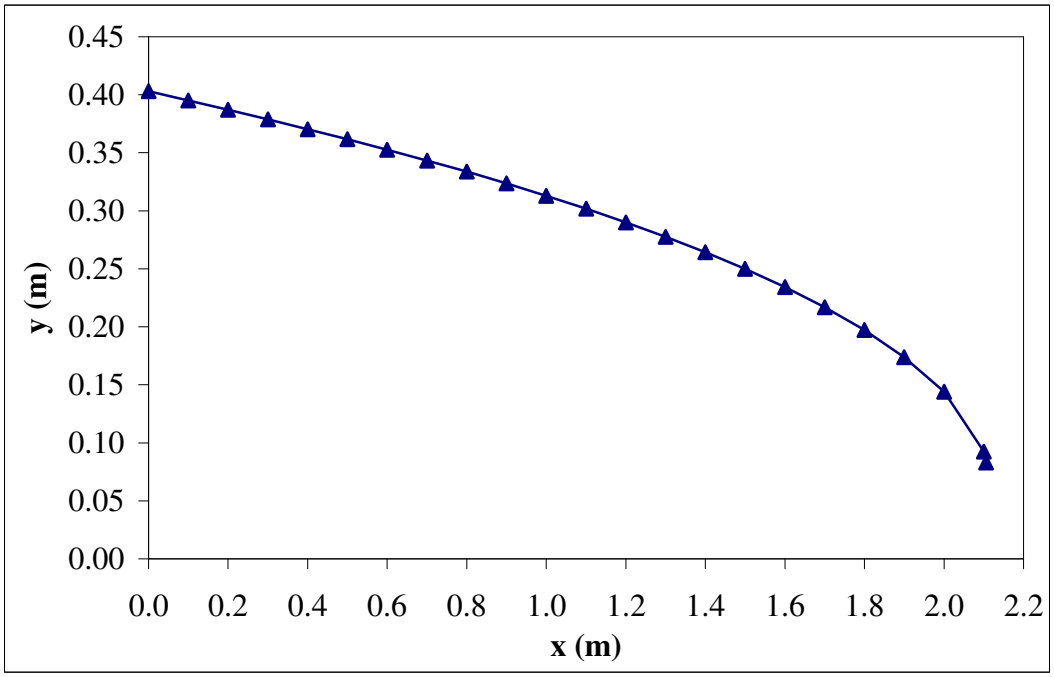

Figure A.10 Water surface profile calculated numerically for experiment 6

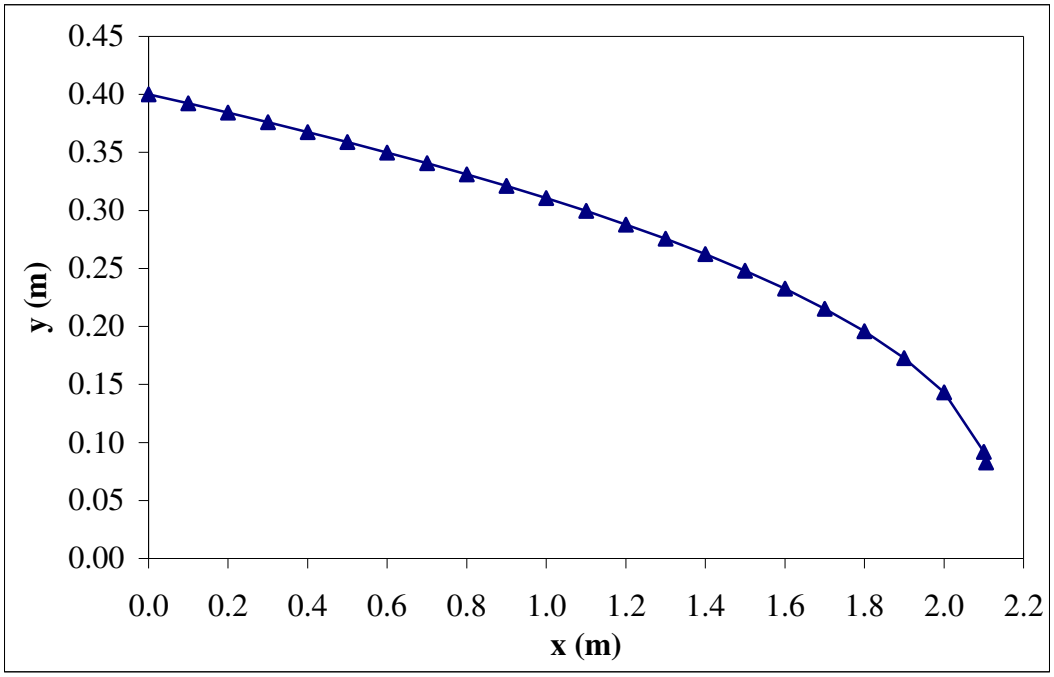

Figure A.11 Water surface profile calculated numerically for experiment 7

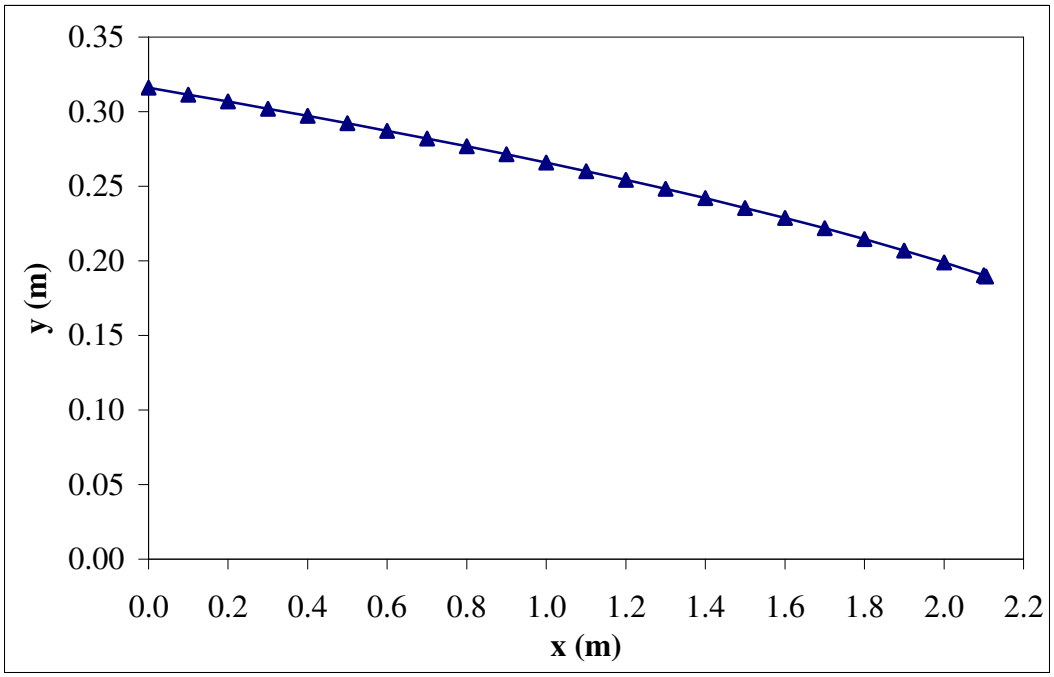

Figure A.12 Water surface profile calculated numerically for experiment 8

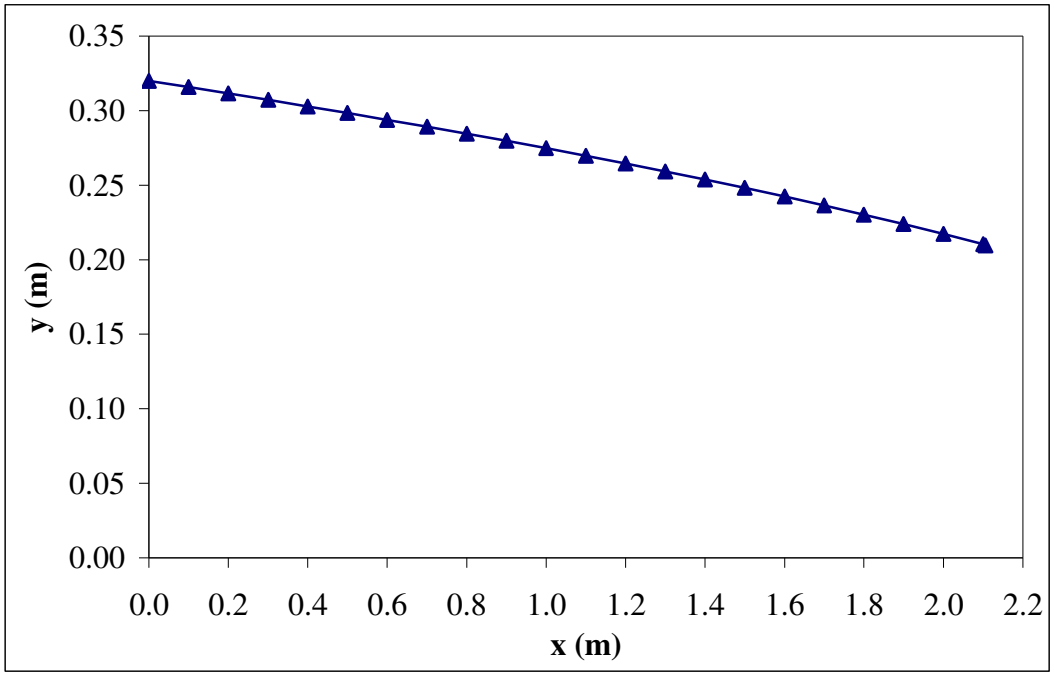

Figure A.13 Water surface profile calculated numerically for experiment 9

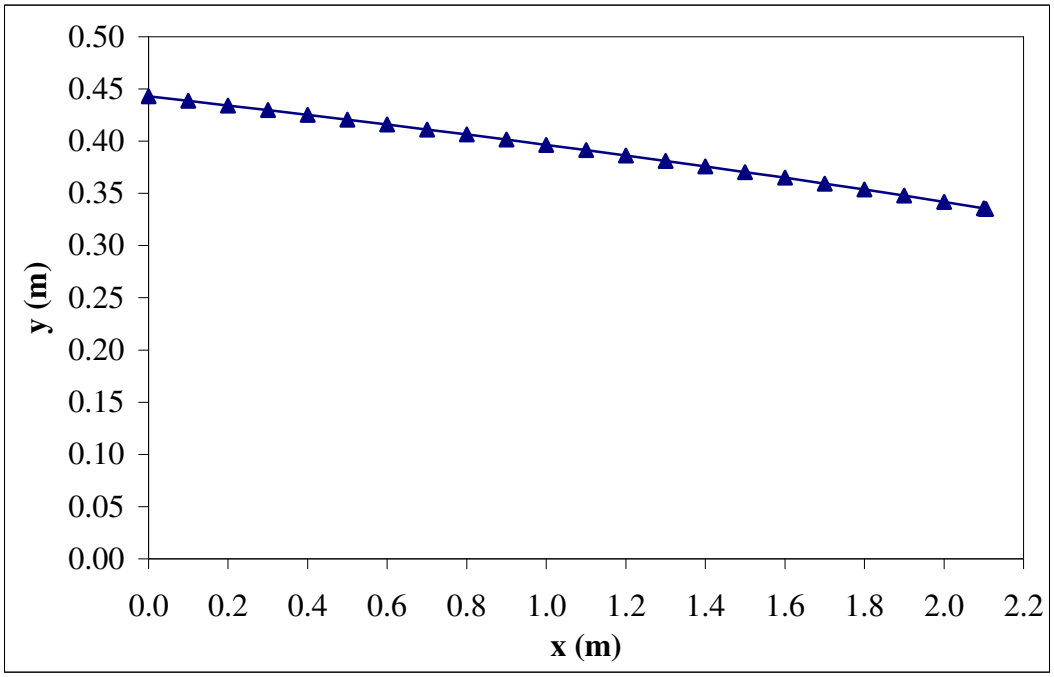

Figure A.14 Water surface profile calculated numerically for experiment 10

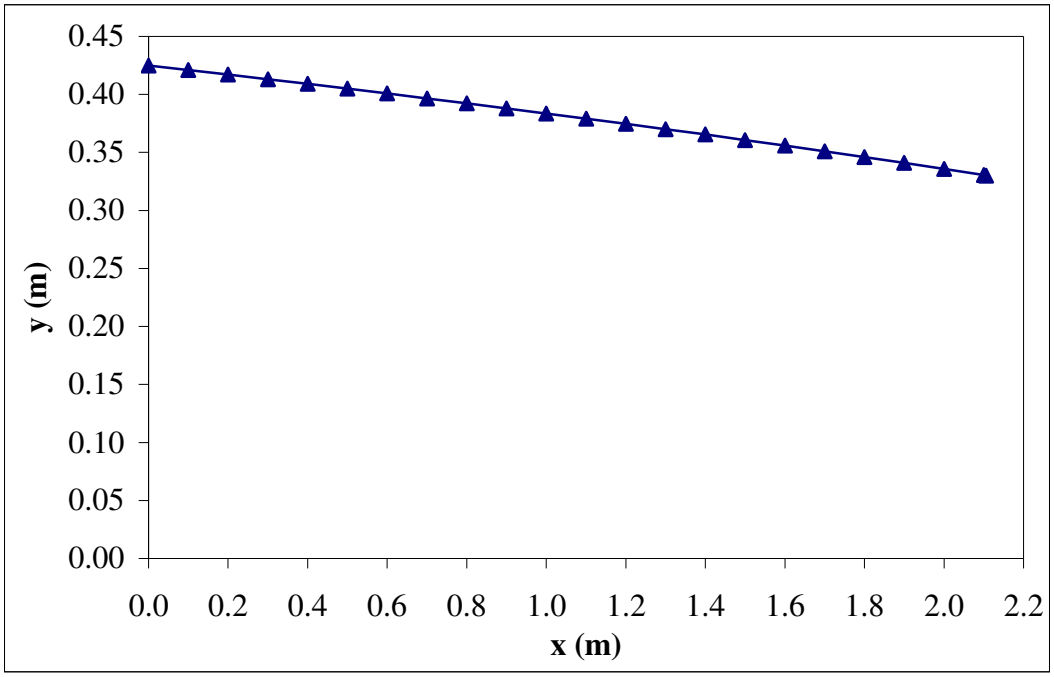

Figure A.15 Water surface profile calculated numerically for experiment 11

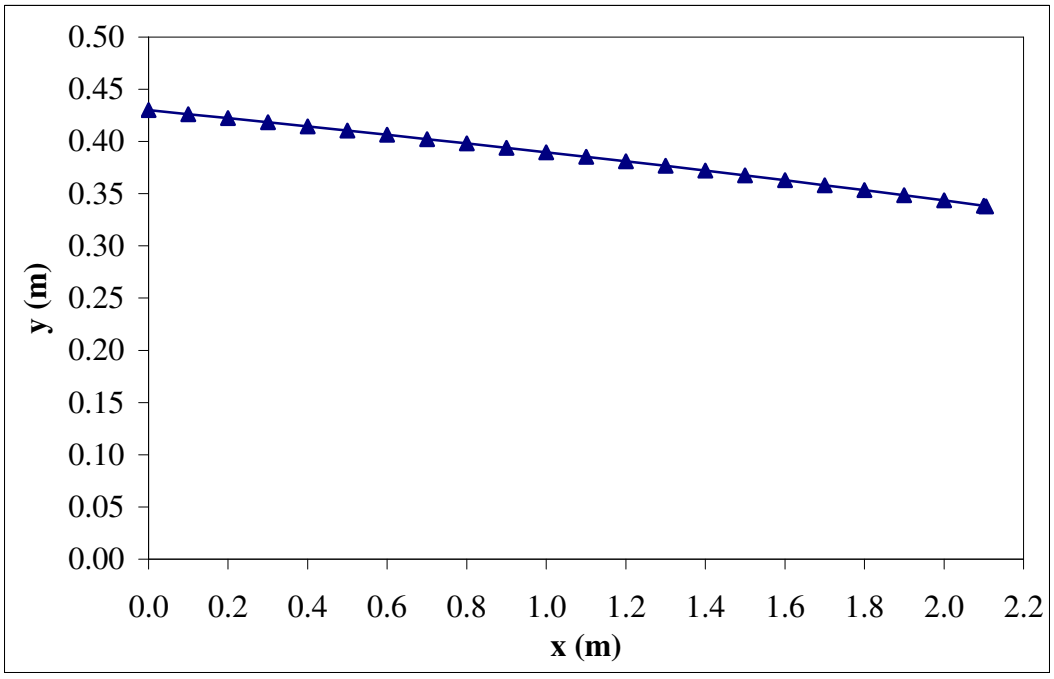

Figure A.16 Water surface profile calculated numerically for experiment 12

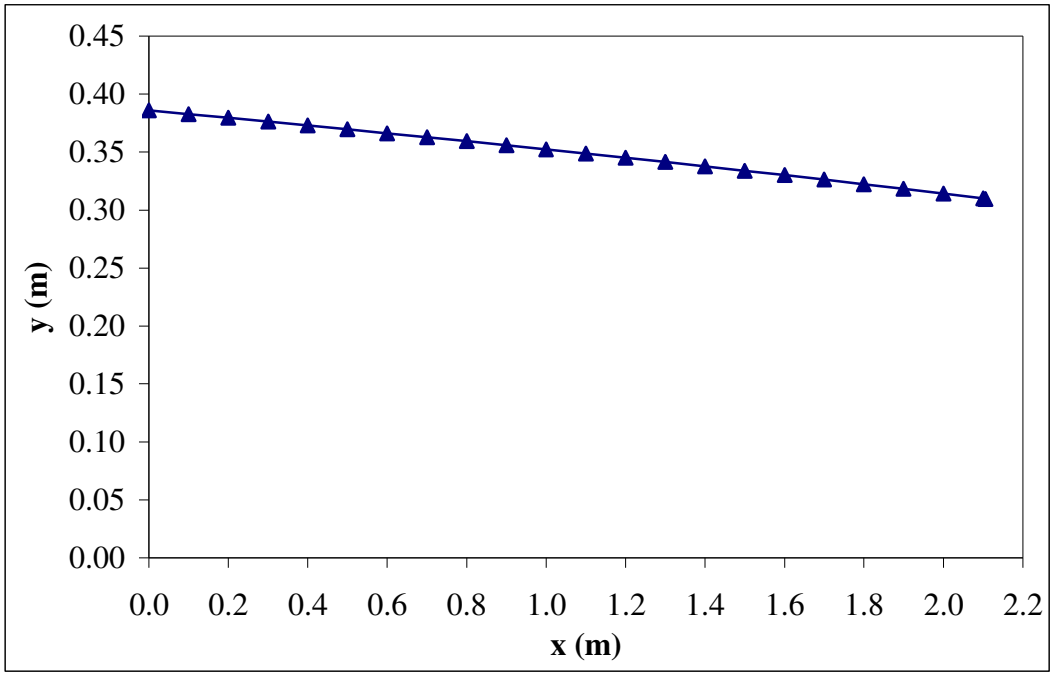

Figure A.17 Water surface profile calculated numerically for experiment 13

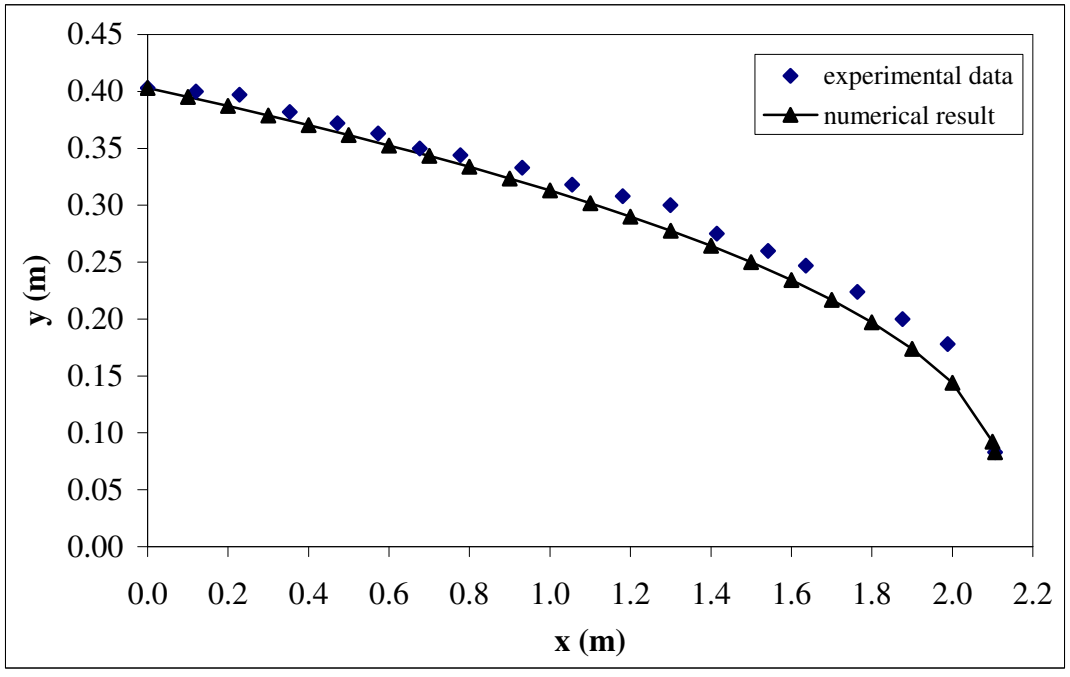

Figure A.18 Comparison of numerical and experimental data for experiment 6

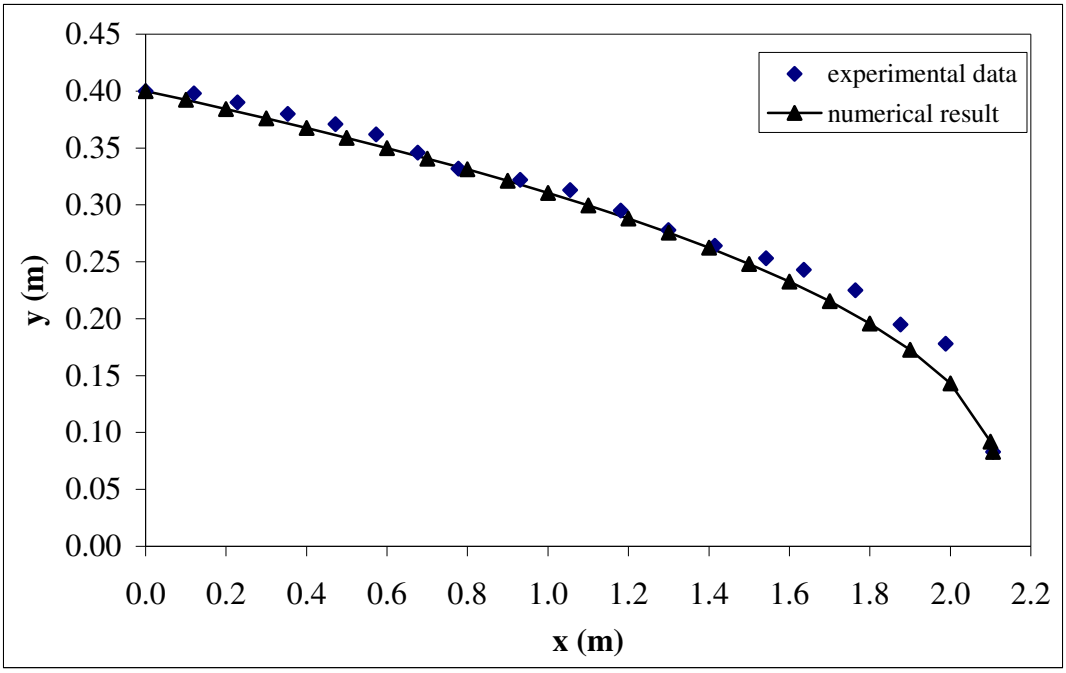

Figure A.19 Comparison of numerical and experimental data for experiment 7

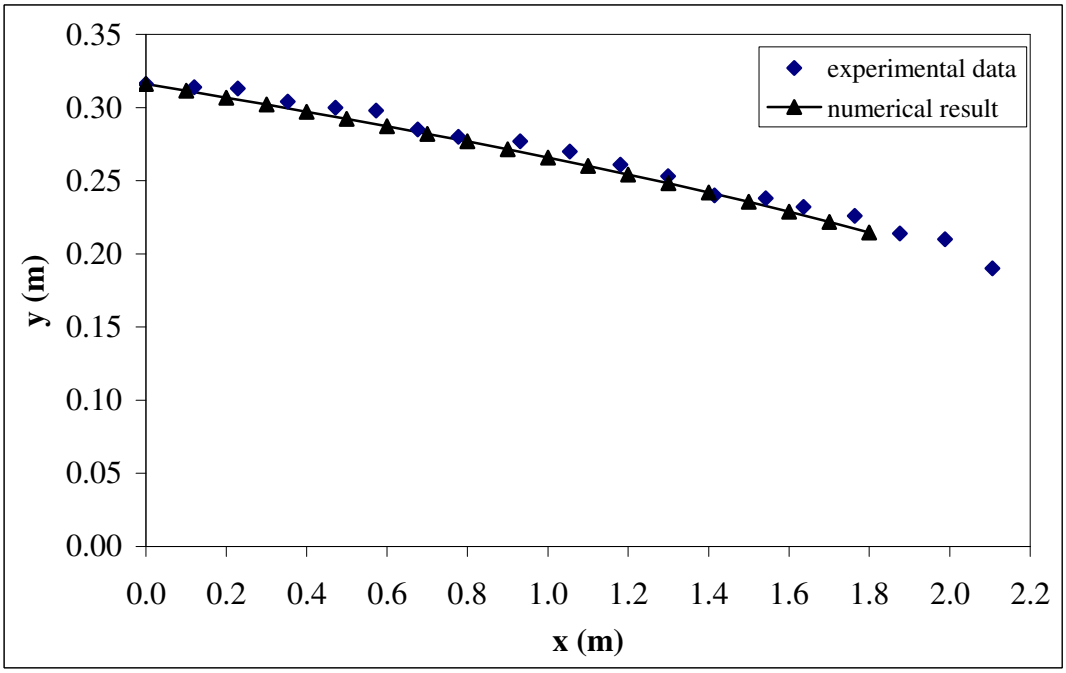

Figure A.20 Comparison of numerical and experimental data for experiment 8

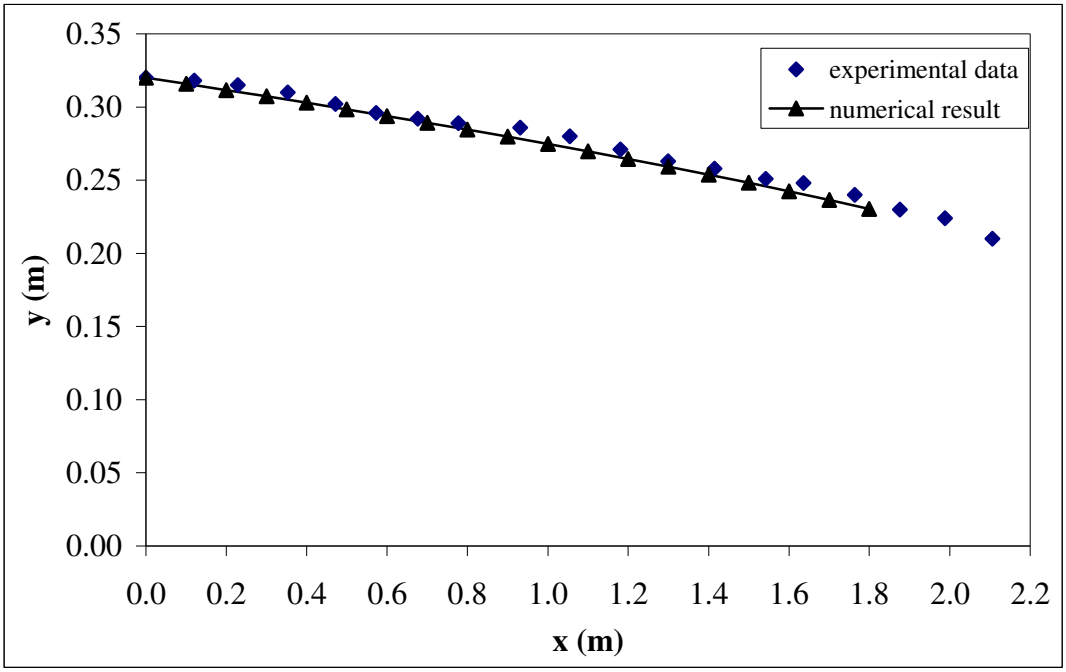

Figure A.21 Comparison of numerical and experimental data for experiment 9

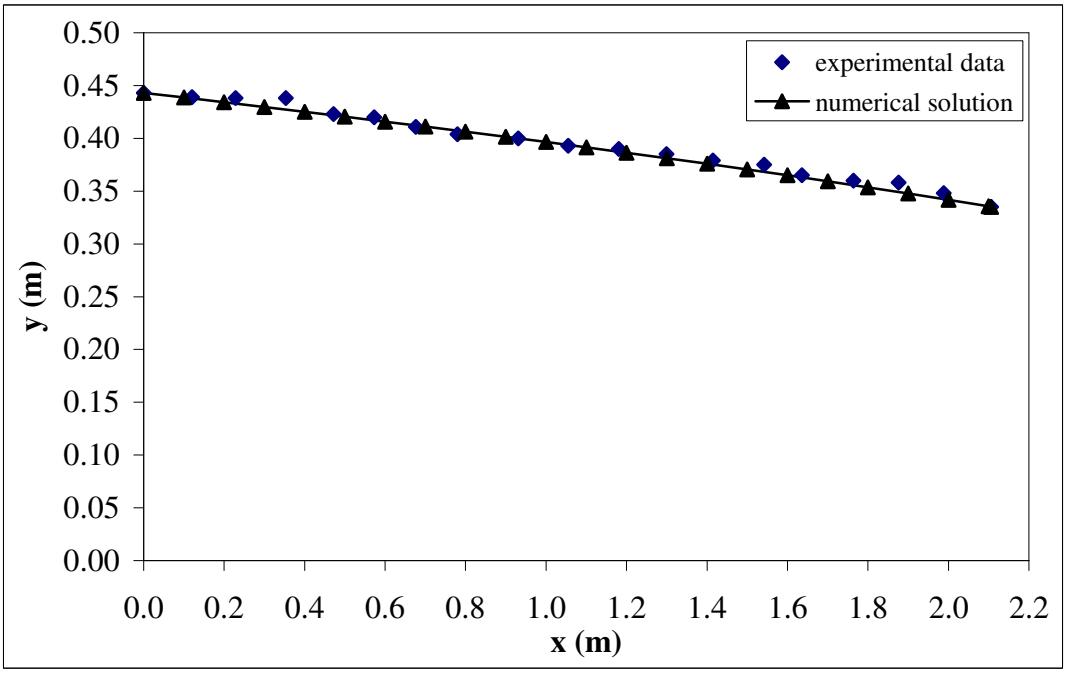

Figure A.22 Comparison of numerical and experimental data for experiment 10

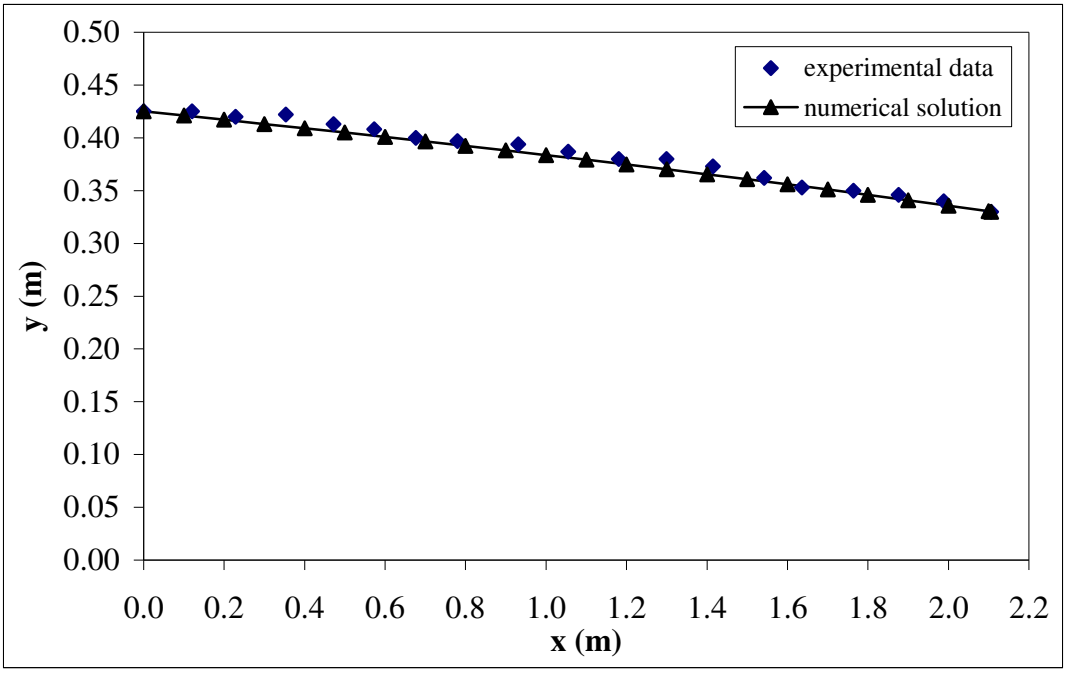

Figure A.23 Comparison of numerical and experimental data for experiment 11

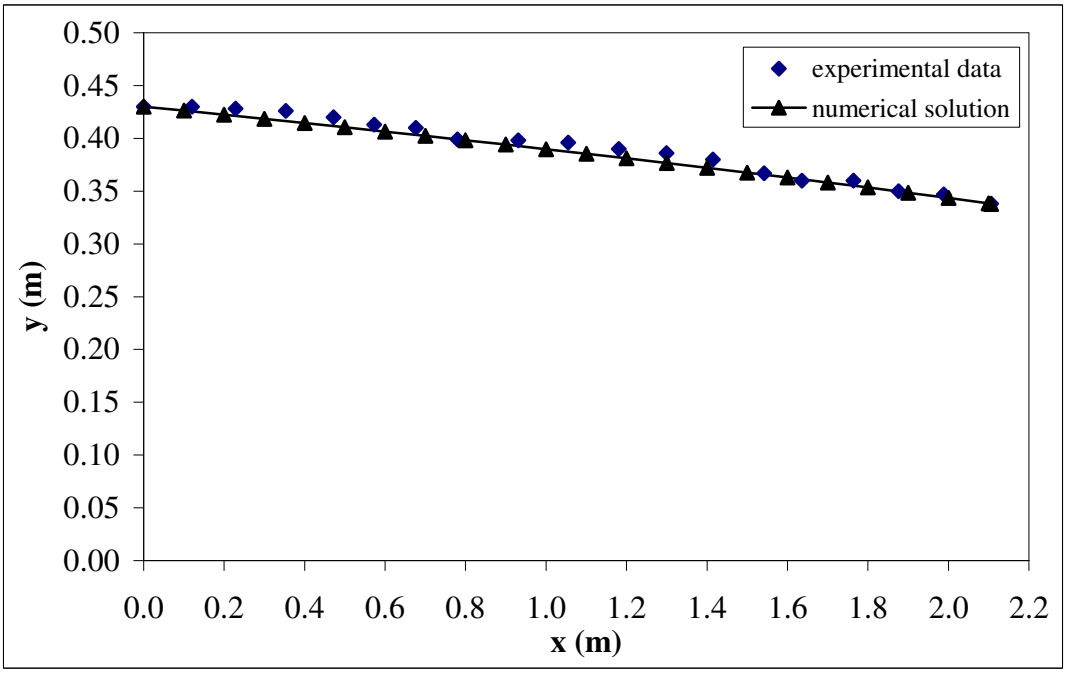

Figure A.24 Comparison of numerical and experimental data for experiment 12

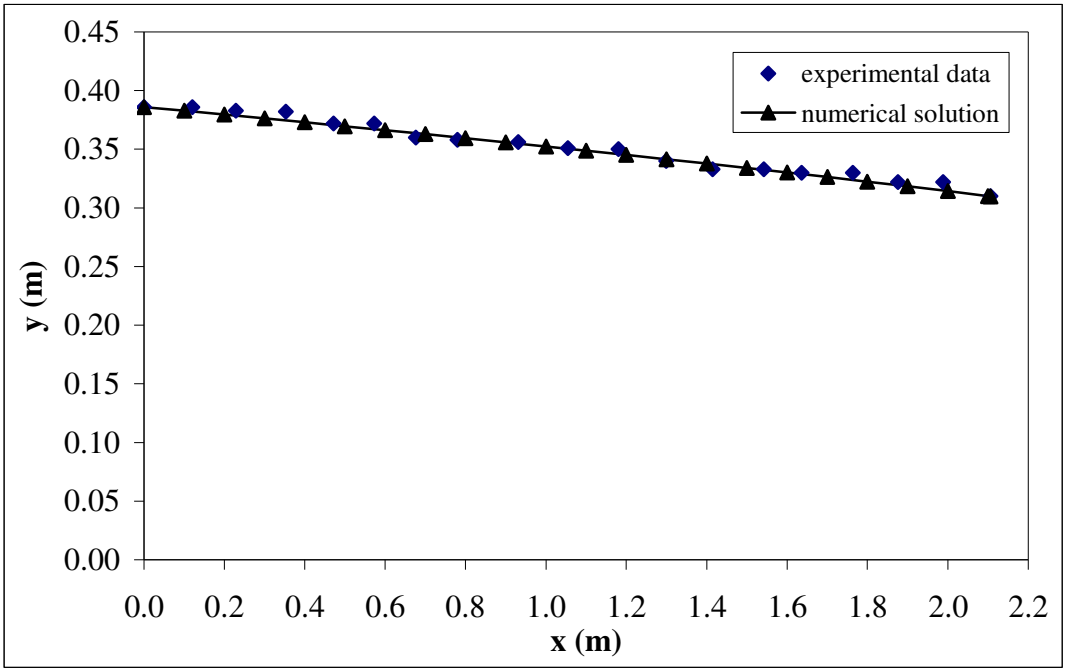

Figure A.25 Comparison of numerical and experimental data for experiment 13

Table A.1 Water head elevations determined by experiments 1 to 6

x (m)	y_{exp1} (m)	y_{exp2} (m)	y_{exp3} (m)	y_{exp4} (m)	y_{exp5} (m)	y_{exp6} (m)
0.000	0.350	0.370	0.375	0.421	0.480	0.403
0.120	0.349	0.369	0.375	0.415	0.480	0.400
0.228	0.348	0.368	0.373	0.410	0.470	0.397
0.353	0.345	0.366	0.372	0.404	0.470	0.382
0.472	0.343	0.364	0.371	0.397	0.465	0.372
0.573	0.341	0.361	0.370	0.390	0.460	0.363
0.676	0.338	0.360	0.368	0.372	0.456	0.350
0.777	0.337	0.358	0.367	0.367	0.452	0.344
0.931	0.334	0.355	0.366	0.355	0.441	0.333
1.055	0.332	0.353	0.364	0.350	0.430	0.318
1.181	0.329	0.352	0.362	0.335	0.420	0.308
1.299	0.327	0.350	0.360	0.327	0.418	0.300
1.415	0.324	0.346	0.358	0.320	0.408	0.275
1.542	0.320	0.343	0.357	0.300	0.400	0.260
1.636	0.318	0.342	0.356	0.290	0.387	0.247
1.764	0.316	0.339	0.355	0.280	0.380	0.224
1.876	0.314	0.337	0.353	0.260	0.370	0.200
1.988	0.314	0.337	0.351	0.253	0.363	0.178
2.106	0.311	0.335	0.350	0.213	0.350	0.083

Table A.2 Water head elevations determined by experiments 7 to 13

x (m)	y_{exp7} (m)	y_{exp8} (m)	y_{exp9} (m)	y_{exp10} (m)	y_{exp11} (m)	y_{exp12} (m)	y_{exp13} (m)
0.000	0.400	0.316	0.320	0.443	0.425	0.430	0.386
0.120	0.398	0.314	0.318	0.439	0.425	0.430	0.386
0.228	0.390	0.313	0.315	0.438	0.420	0.428	0.383
0.353	0.380	0.304	0.310	0.438	0.422	0.426	0.382
0.472	0.371	0.300	0.302	0.423	0.413	0.420	0.372
0.573	0.362	0.298	0.296	0.420	0.408	0.413	0.372
0.676	0.346	0.285	0.292	0.411	0.400	0.410	0.360
0.777	0.332	0.280	0.289	0.404	0.397	0.399	0.358
0.931	0.322	0.277	0.286	0.400	0.394	0.398	0.356
1.055	0.313	0.270	0.280	0.393	0.387	0.396	0.351
1.181	0.295	0.261	0.271	0.390	0.380	0.390	0.350
1.299	0.278	0.253	0.263	0.385	0.380	0.386	0.340
1.415	0.264	0.240	0.258	0.379	0.373	0.380	0.333
1.542	0.253	0.238	0.251	0.375	0.362	0.367	0.333
1.636	0.243	0.232	0.248	0.365	0.353	0.360	0.330
1.764	0.225	0.226	0.240	0.360	0.350	0.360	0.330
1.876	0.195	0.214	0.230	0.358	0.346	0.350	0.322
1.988	0.178	0.210	0.224	0.348	0.340	0.347	0.322
2.106	0.083	0.190	0.210	0.335	0.330	0.338	0.310

Table A.3 Discharge measurements for experiments 1 to 6

Exp. No	1	2	3	4	5	6
H =	0.80	0.78	0.75	2.30	2.10	2.30
C_d =	0.732	0.735	0.740	0.655	0.658	0.655
Q (m^3/s) =	0.00101	0.00097	0.00092	0.00438	0.00384	0.00438
Q (lt/s) =	1.0055	0.9722	0.92298	4.38276	3.84478	4.38276
Q (m^3/day) =	86.878	84.001	79.745	378.670	332.189	378.670

Table A.4 Discharge measurements for experiments 7 to 13

Exp. No	7	8	9	10	11	12	13
H =	2.25	1.30	1.20	1.80	1.80	1.80	1.40
C_d =	0.655	0.685	0.692	0.665	0.665	0.665	0.680
Q (m^3/s) =	0.00425	0.00195	0.00174	0.00308	0.00308	0.00308	0.00216
Q (lt/s) =	4.24602	1.94995	1.74484	3.08414	3.08414	3.08414	2.16260
Q (m^3/day) =	366.856	168.476	150.755	266.470	266.470	266.470	186.849

Table A.5 Water head elevations computed numerically for experiments 1 to 6

x (m)	y_{exp1} (m)	y_{exp2} (m)	y_{exp3} (m)	y_{exp4} (m)	y_{exp5} (m)	y_{exp6} (m)
0.000	0.350	0.370	0.375	0.421	0.480	0.403
0.100	0.348	0.368	0.374	0.414	0.475	0.395
0.200	0.346	0.367	0.373	0.407	0.470	0.387
0.300	0.345	0.365	0.372	0.400	0.464	0.379
0.400	0.343	0.364	0.370	0.393	0.459	0.370
0.500	0.341	0.362	0.369	0.385	0.453	0.362
0.600	0.339	0.360	0.368	0.377	0.448	0.353
0.700	0.338	0.359	0.367	0.370	0.442	0.343
0.800	0.336	0.357	0.366	0.361	0.437	0.334
0.900	0.334	0.356	0.365	0.353	0.431	0.324
1.000	0.332	0.354	0.363	0.344	0.425	0.313
1.100	0.330	0.352	0.362	0.335	0.419	0.302
1.200	0.328	0.351	0.361	0.326	0.413	0.290
1.300	0.327	0.349	0.360	0.316	0.406	0.278
1.400	0.325	0.347	0.359	0.306	0.400	0.264
1.500	0.323	0.346	0.357	0.295	0.393	0.250
1.600	0.321	0.344	0.356	0.284	0.387	0.234
1.700	0.319	0.342	0.355	0.272	0.380	0.217
1.800	0.317	0.340	0.354	0.260	0.373	0.197
1.900	0.315	0.339	0.353	0.246	0.366	0.174
2.000	0.313	0.337	0.351	0.231	0.358	0.144
2.100	0.311	0.335	0.350	0.215	0.351	0.092
2.106	0.311	0.335	0.350	0.213	0.350	0.083

Table A.6 Water head elevations computed numerically for experiments 7 to 13

x (m)	y_{exp7} (m)	y_{exp8} (m)	y_{exp9} (m)	y_{exp10} (m)	y_{exp11} (m)	y_{exp12} (m)	y_{exp13} (m)
0.000	0.400	0.316	0.320	0.443	0.425	0.430	0.386
0.100	0.392	0.311	0.316	0.439	0.421	0.426	0.383
0.200	0.384	0.307	0.312	0.434	0.417	0.422	0.380
0.300	0.376	0.302	0.307	0.430	0.413	0.418	0.376
0.400	0.368	0.297	0.303	0.425	0.409	0.414	0.373
0.500	0.359	0.292	0.298	0.421	0.405	0.410	0.370
0.600	0.350	0.287	0.294	0.416	0.401	0.406	0.366
0.700	0.341	0.282	0.289	0.411	0.397	0.402	0.363
0.800	0.331	0.277	0.285	0.406	0.392	0.398	0.359
0.900	0.321	0.271	0.280	0.401	0.388	0.394	0.356
1.000	0.311	0.266	0.275	0.397	0.384	0.390	0.352
1.100	0.300	0.260	0.270	0.391	0.379	0.385	0.349
1.200	0.288	0.254	0.265	0.386	0.375	0.381	0.345
1.300	0.275	0.248	0.259	0.381	0.370	0.377	0.341
1.400	0.262	0.242	0.254	0.376	0.365	0.372	0.338
1.500	0.248	0.235	0.248	0.370	0.361	0.368	0.334
1.600	0.233	0.229	0.242	0.365	0.356	0.363	0.330
1.700	0.215	0.222	0.236	0.359	0.351	0.358	0.326
1.800	0.196	0.215	0.230	0.354	0.346	0.353	0.322
1.900	0.173	0.207	0.224	0.348	0.341	0.349	0.318
2.000	0.143	0.199	0.217	0.342	0.336	0.344	0.314
2.100	0.092	0.190	0.210	0.336	0.331	0.339	0.310
2.106	0.083	0.189	0.210	0.335	0.330	0.338	0.310

The computation process of modeling flow through porous media by using Stephenson equation is provided by the flow chart shown in Figure A.26 and step-by-step explanation is given below.

Step 1. Start. Rockfill parameters, channel properties, identification of constants, and initial water depth y_0 are inserted.

Step 2. Start iteration from known water depth y_i

Step 3. Calculate $(dy/dx)_i$ using Equation (2.19);

Step 4. Assume $(dy/dx)_{i+1} = (dy/dx)_i$;

Step 5. Calculate y_{i+1}^{j} using Equation (3.5);

Step 6. Calculate $(dy/dx)_{i+1}^{j}$ using y_{i+1}^{j} ;

Step 7. Calculate y_{i+1}^{j+1} using Equation (3.7);

Step 8. Check $\varepsilon = \left| \frac{y_{i+1}^{j+1} - y_{i+1}^{j}}{y_{i+1}^{j}} \right| \leq 10^{-7}$;

Step 9. If not, go to *Step 6* with assuming $y_{i+1}^{j} = y_{i+1}^{j+1}$;

yes, stop iteration;

Step 10. Result, $y_{i+1} = y_{i+1}^{j+1}$

Step 11. Check if $i+1=N$; not go to *Step 2* with assuming $y_i = y_{i+1}$;

otherwise, STOP.

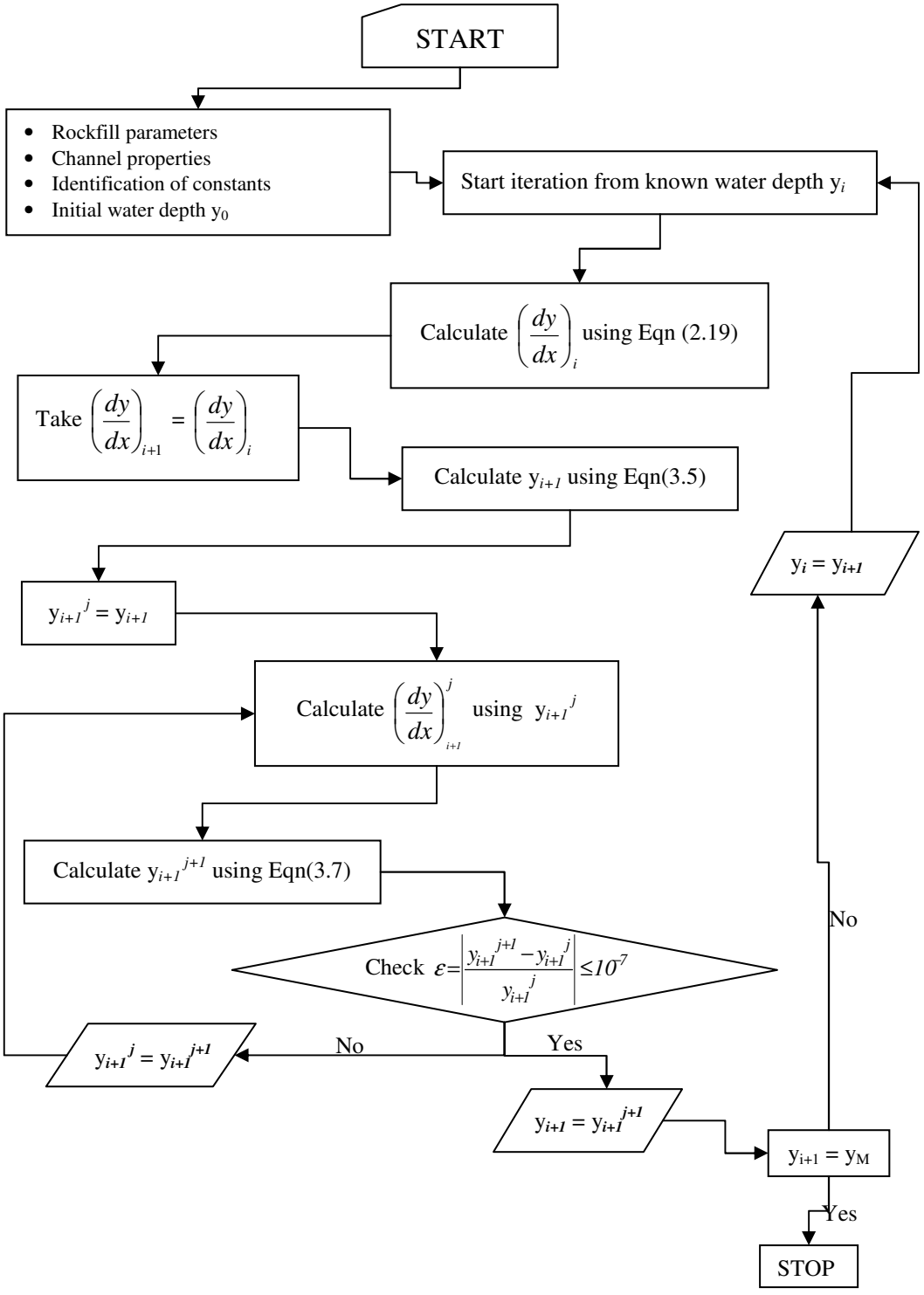

Figure A.26 Flow chart used in computation of water surface profile by using Stephenson relation

The computation process of modeling flow through porous media by using Wilkins equation is provided by the flow chart shown in Figure A.27 and step-by-step explanation is given below.

Step 1. Start. Rockfill parameters, channel properties, identification of constants, and initial water depth y_0 are inserted.

Step 2. Start iteration from known water depth y_i

Step 3. Calculate $(dy/dx)_i$ using Equation (2.20);

Step 4. Assume $(dy/dx)_{i+1} = (dy/dx)_i$;

Step 5. Calculate y_{i+1}^{j} using Equation (3.5);

Step 6. Calculate $(dy/dx)_{i+1}^{j}$ using y_{i+1}^{j} ;

Step 7. Calculate y_{i+1}^{j+1} using Equation (3.8);

Step 8. Check $\varepsilon = \left| \frac{y_{i+1}^{j+1} - y_{i+1}^{j}}{y_{i+1}^{j}} \right| \leq 10^{-7}$;

Step 9. If not, go to *Step 6* with assuming $y_{i+1}^{j} = y_{i+1}^{j+1}$;

yes, stop iteration;

Step 10. Result, $y_{i+1} = y_{i+1}^{j+1}$

Step 11. Check if $i+1=N$; not go to *Step 2* with assuming $y_i = y_{i+1}$;

otherwise, STOP.

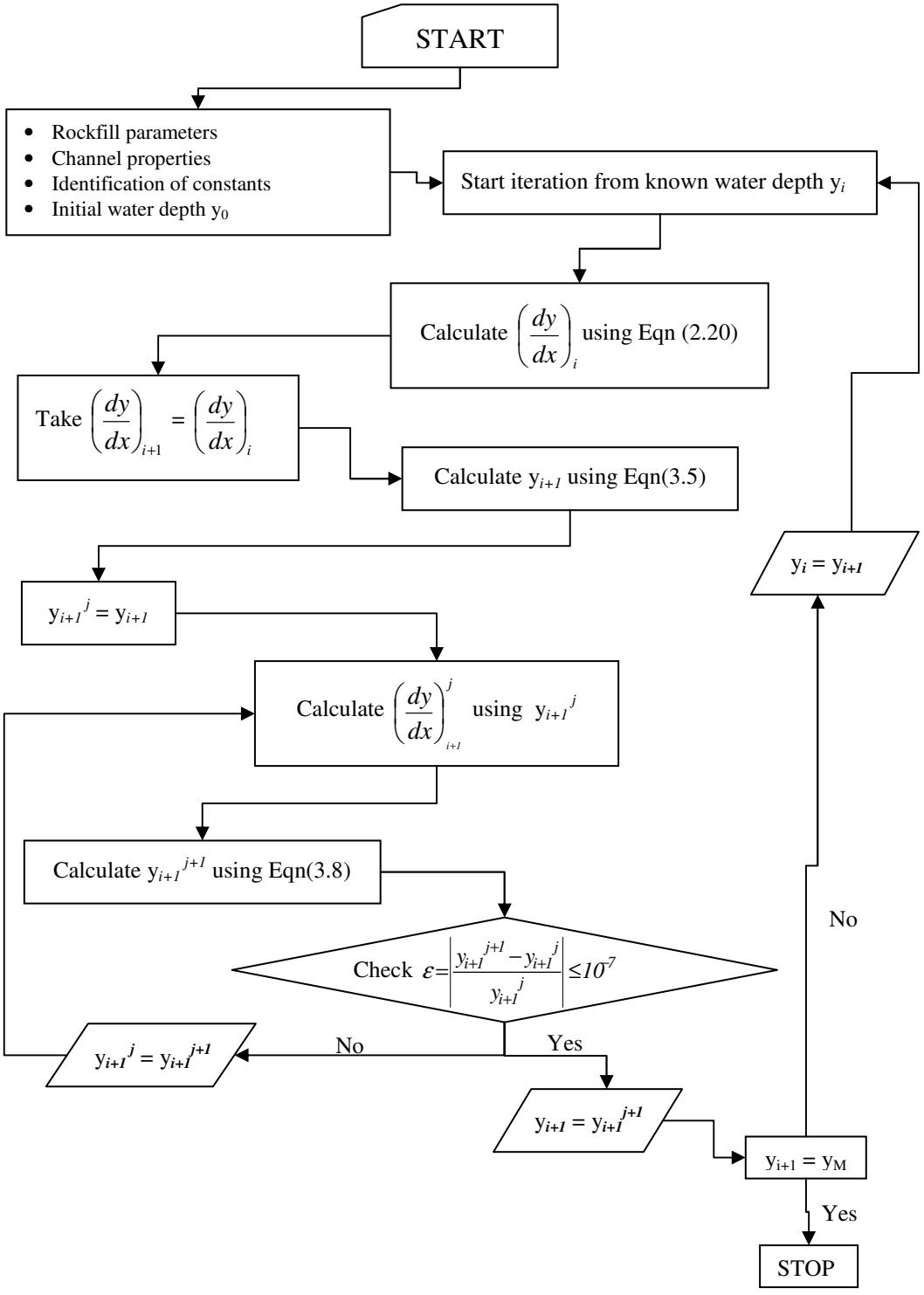

Figure A.27 Flow chart used in computation of water surface profile by using Wilkins relation

APPENDIX B

PHOTOGRAPHS FROM EXPERIMENTS

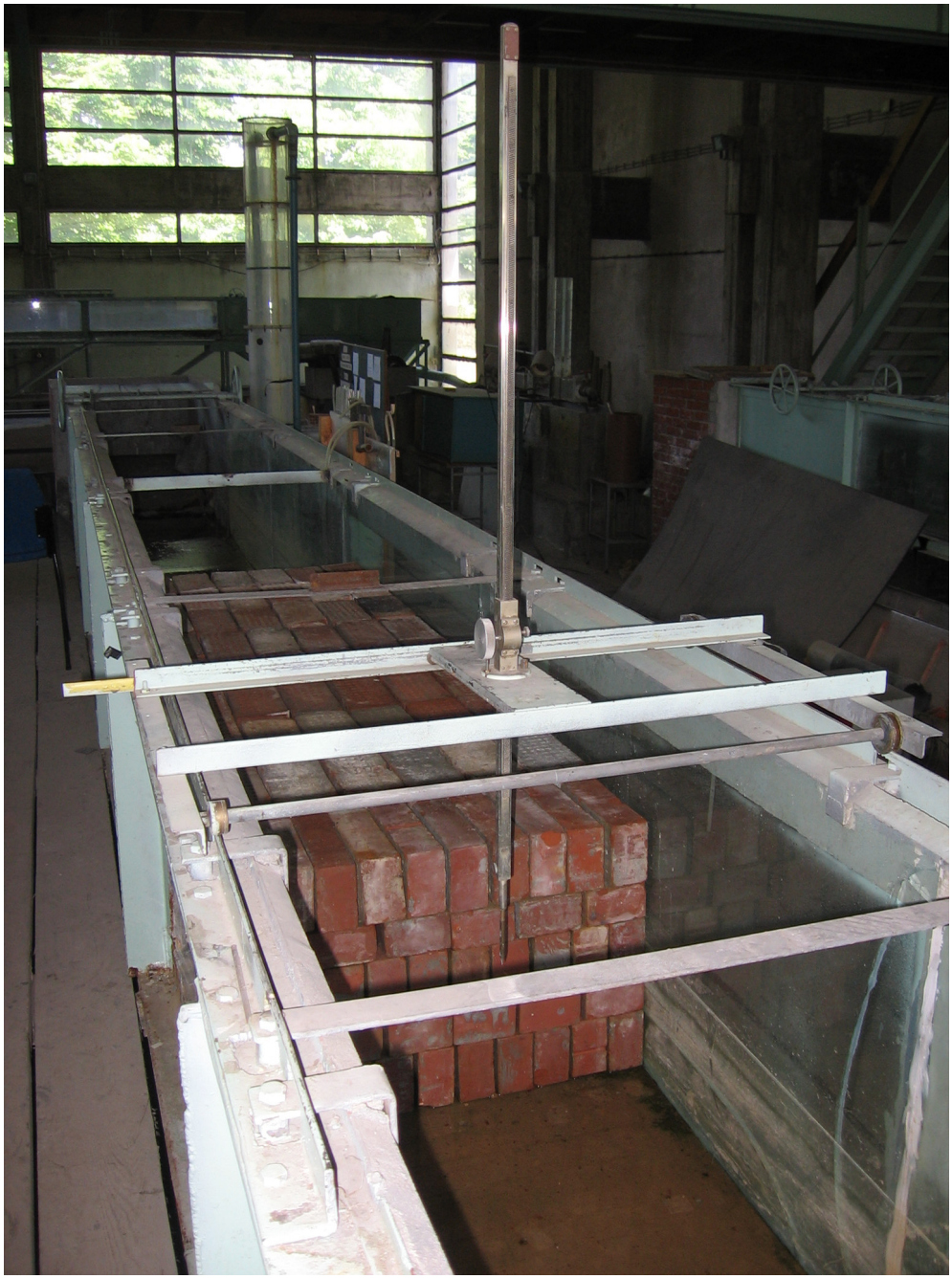

Figure B.1 Upstream view of the experimental setup

Figure B.2 Frontal view of the weir model

Figure B.3 Backward view of the weir model

Figure B.4 Flap gate installed at downstream

Figure B.5 Downstream view of the experimental setup

Figure B.6 Side view of the weir model with measuring points

Figure B.7 Side view of the channel